SANDIA REPORT
SAND2009-2173
Unlimited Release
Printed October 2009

Quantifying Reliability Uncertainty: A Proof of Concept

John F. Lorio, Michael A. Dvorack, Michael J. Mundt, Kathleen V. Diegert,
James T. Ringland, and Rena Zurn
Sandia National Laboratories

Christine Anderson-Cook, Aparna Huzurbazar, Alyson Wilson, and Quinn Fatherley
Los Alamos National Laboratory

Prepared by
Sandia National Laboratories
Albuquerque, New Mexico 87185 and Livermore, California 94550

Sandia is a multiprogram laboratory operated by Sandia Corporation,
a Lockheed Martin Company, for the United States Department of Energy's
National Nuclear Security Administration under Contract DE-AC04-94AL85000.

Statistical Sciences Group, Los Alamos National Laboratory, Los Alamos, NM 87545.
This work was supported by Enhanced Surveillance Campaign (C8) and Joint Munitions Program. This work was performed under the auspices of the Los Alamos National Laboratory, an affirmative action/equal opportunity employer, operated by the Los Alamos National Security, LLC, for the National Nuclear Security Administration of the U.S. Department of Energy under contract DE-AC52-06NA25396.

Issued by Sandia National Laboratories, operated for the United States Department of Energy by Sandia Corporation.

Available to DOE and DOE contractors from
U.S. Department of Energy
Office of Scientific and Technical Information
P.O. Box 62
Oak Ridge, TN 37831

Telephone: (865) 576-8401
Facsimile: (865) 576-5728
E-Mail: reports@adonis.osti.gov
Online ordering: http://www.osti.gov/bridge

Available to the public from
U.S. Department of Commerce
National Technical Information Service
5285 Port Royal Rd.
Springfield, VA 22161

Telephone: (800) 553-6847
Facsimile: (703) 605-6900
E-Mail: orders@ntis.fedworld.gov
Online order: http://www.ntis.gov/help/ordermethods.asp?loc=7-4-0#online

SAND2009-2173
Unlimited Release
Printed October 2009

Quantifying Reliability Uncertainty: A Proof of Concept*

John Lorio
B61 System Engineering

Mike Dvorack, Mike Mundt, and Kathleen Diegert
Reliability Assessment and Human System Integration

James Ringland and Rena Zurn
Reliability and Electrical Systems

Sandia National Laboratories
P.O. Box 5800
Albuquerque, New Mexico 87185-0447

Christine Anderson-Cook, Aparna Huzurbazar, and Alyson Wilson
Statistical Sciences Group

Quinn Fatherley
Surveillance Oversight

Los Alamos National Laboratory
Los Alamos, New Mexico 87545

Abstract

This paper develops Classical and Bayesian methods for quantifying the uncertainty in reliability for a system of mixed series and parallel components for which both go/no-go and variables data are available. Classical methods focus on uncertainty due to sampling error. Bayesian methods can explore both sampling error and other knowledge-based uncertainties. To date, the reliability community has focused on qualitative statements about uncertainty because there was no consensus on how to quantify them. This paper provides a proof of concept that workable, meaningful quantification methods can be constructed. In addition, the application of the methods demonstrated that the results from the two fundamentally different approaches can be quite comparable. In both approaches, results are sensitive to the details of how one handles components for which no failures have been seen in relatively few tests.

* This is joint work between Sandia National Laboratories and Los Alamos National Laboratory. LANL work is funded by the Enhanced Surveillance Campaign and the DoD/DOE Joint Munitions Program.

TABLE OF CONTENTS

LIST OF FIGURES

LIST OF TABLES

EXECUTIVE SUMMARY

This paper demonstrates a proof of concept of two methods for estimating system-level reliability uncertainty using component-level data. The case study demonstrates the analysis and methods comparison in a common invented system model of a complexity representative of the top-level models used by Sandia National Laboratories and Los Alamos National Laboratory to assess weapon reliability. The study included created data sets.

The first method is a Classical (frequentist) approach that captures and aggregates sampling uncertainties at the component level. The method evaluates the mean and variance of the various component-level reliability estimators and then propagates these through the system-level reliability equation to get an approximate value for the mean and variance of the system reliability estimator. This is used to construct a 90% confidence interval for the system reliability.

The second method is a Bayesian approach that uses Markov Chain Monte Carlo (MCMC) methods to develop the system-level distribution for reliability. The approach selects a user-specified diffuse prior distribution for each component, which is updated based upon the data sets to develop the posterior distribution. By this mechanism, both sampling and other knowledge uncertainties can be captured, although the specific example here emphasizes the former. The individual component-level reliability estimates are then combined to obtain the system-level reliability estimate with an associated uncertainty propagated from the component distributions. This approach is used to construct a 90% credible interval for system reliability.

Although the two approaches have significant conceptual differences, in the case study explored the two gave closely comparable results. Both methods prove to be sensitive to how they handle component reliability evaluation when no failures in relatively few trials are observed. This sensitivity can be much larger than the differences between Classical and Bayesian formulations.

Figure ES-1 illustrates both this close comparability and sensitivity to the details of handling of zero-failure cases. This figure gives the 90% Classical confidence intervals and 90% Bayesian credible intervals in two different cases where different underlying assumptions were made concerning the handling of zero-failure cases.

The left side shows results when both the Classical and Bayesian approaches use a reliability of "1" for two influential components, identified in the model as "J1E" and "J4E." There is no data associated with the first; all uncertainty is knowledge-based. There are no failures in 106 trials associated with the second. Note the intervals are quite comparable. In the Classical formulation as applied here, a best-estimate reliability of "1" naturally associates with no uncertainty whereas the Bayesian approach has the usual flexibility to account for associated uncertainty through a prior distribution.

The right side explores another pair of alternatives for the zero-failure cases. Here the Classical formulation uses the 50% upper confidence limit for the best estimate of the J4E failure probability and associates that estimator with a variation on a binomial distribution. The

Classical formulation does not deal with pure knowledge uncertainties, so JE1 is still treated as having a fixed reliability of "1." The second Bayesian approach incorporates uncertainty for J4E from a diffuse prior and for JE1, which represents epistemic uncertainty, by a beta distribution formulated based from expert elicitation. The intervals are wider than their left-side counterparts by comparable amounts. The Bayesian credible interval has a smaller value for its lower bound because it includes effects of JE1 while the Classical one cannot.

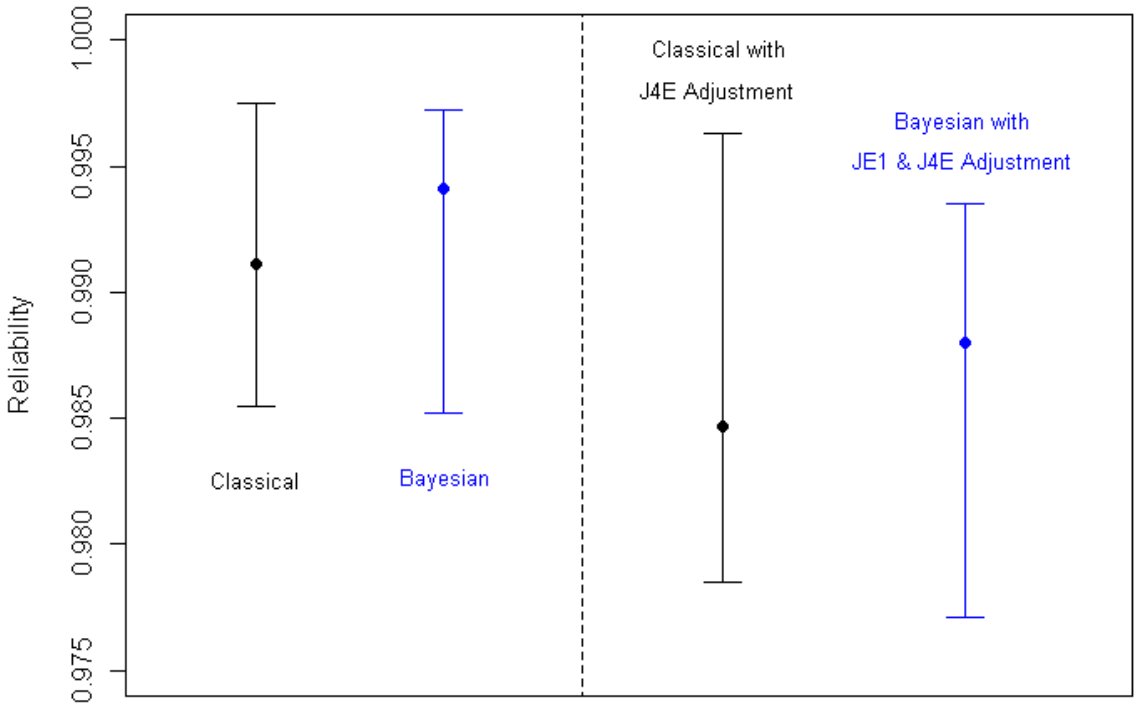

Figure ES-1. Comparison of Bayesian and Classical approaches in estimating reliability and uncertainty.

From the development of the two methods and comparison of their application to the sample problem, it is possible to draw several other comparisons and observations.

The different handling of J1E above illustrates the difference in the logical scope of the uncertainties that can be considered by the two approaches. The Classical approach to uncertainty only deals with sampling uncertainty. The Bayesian methods capture this as well as a measure of knowledge uncertainties.

The Bayesian calculation can show some sensitivity to assumptions about component and system reliabilities captured in the prior distributions. This might cause significant differences between the two approaches and lower credible interval estimates. However, the choice of an appropriate prior does allow for knowledge about the component or system separate from the data to be included. In a real study, considerable time would be spent in choosing appropriate priors for the Bayesian approach using methods such as expert elicitation.

The Classical calculation relies on some rather specific statistical assumptions needed to fold the probability distributions for the component reliability estimators into a distribution of the system estimator. There may well be considerable sensitivity there. In a real study, time would need to be spent understanding the impact of these specific assumptions.

Both approaches start from a small number of basic principles but then require a fair amount of mathematical machinery to execute. Both can be complex. In the Classical case, much of the complexity involves the analytic manipulation of the equations. For more complex problems than the one here, however, some of this might be done numerically (e.g., numerical computation of the derivatives needed for the mean and variance expansions). In the Bayesian case, more of the analysis was done numerically, and the underlying use of MCMC is both sophisticated and computation-intensive.

For this proof-of-concept case study, our focus is on demonstrating that these types of calculations can be performed on complex systems rather than aiming for a one-to-one comparison between the Classical and Bayesian approaches. We were gratified that the results demonstrated substantial similarities, at least for the relatively data-rich example considered here. This is only a first step toward gaining a scientific consensus on methods. More work would be required to extend these to a proper decision framework that is not overly simplified. In addition, to appropriately reflect understanding of a real system, more emphasis would be placed on how the priors in the Bayesian method would be selected and how Classical distribution assumptions could be validated.

1. SYSTEM RELIABILITY MODEL AND EXAMPLE DATA

Purpose

The weapons complex gathers the bulk of system reliability and failure mode data at the component level and uses the data to make inferences regarding system reliability. Such data contains both sampling error and other knowledge uncertainties, but currently it is common to report only a single best estimate of reliability. There has not been a consensus on appropriate methods for capturing the effects of sampling and other knowledge uncertainties quantitatively at the component level and for aggregating them into a system-level uncertainty statement. The only approach to date has been to capture special concerns qualitatively: to identify that the best estimate carries "increased uncertainty" or to withhold reporting of reliability because of even larger uncertainty. The decision to cite these special qualitative concerns has been based primarily on knowledge uncertainties due to the lack of current data, which is only one, though arguably the most dominant, of the many sources of uncertainty.

The purpose of this paper is to explore two approaches for capturing and aggregating uncertainty from the component level to the system level. This report was compiled from briefings presented by Sandia National Laboratories (SNL) and Los Alamos National Laboratory (LANL) on their respective approaches.

The first method is a Classical technique, developed by the SNL team, and propagates moments through the reliability estimator to estimate mean and variance of the system reliability. This approach can capture and aggregate sampling uncertainty only, and uses asymptotic approximations to propagate the uncertainty to a system-level summary. Classical approaches need to be embedded into a larger risk-based framework to deal with knowledge-based uncertainties. This is discussed in Ringland et al. (2009).

The second approach, developed by the LANL team, uses a Bayesian Markov Chain Monte Carlo (MCMC) approach to characterize the actual distribution of the system reliability through simulation and sampling. This approach can aggregate both sampling and any broader knowledge uncertainties, such as including expert elicitation, which can be described quantitatively at the component level, although the latter has only limited development here.

Our motivation for this project is to demonstrate a proof of concept that complex system reliability can be estimated with an associated uncertainty measure that captures some, if not all, of the relevant sources of uncertainty. A secondary goal of the methodology is to provide a foundation for building tools to aid in making decisions for deploying testing resources that most reduce uncertainty. SNL explores this aspect in the companion paper by Ringland et al. (2009). LANL has a series of works that develops resource allocation methodology for selecting the best use of new resources to maximally improve the precision of the system reliability estimate (c.f., Wilson et al. 2006; Anderson-Cook et al. 2008 and 2009; Hamada et al. 2008).

Model Reliability Block Diagram

We first defined an example system, with an appropriate degree of resolution and appropriate data. The model in its original form is shown in Figure 1-1, as represented in ReliaSoft software.

This model includes a variety of series/parallel components and is reasonably complex. Blocks represent successful function of one component or component assembly. Two different blocks having the same label, as for example the two blocks labeled K14 near the top, indicate redundant copies of the same sort of component. We created data sets for each of the blocks in the diagram, including some time-dependent data, to simulate complexity that we may expect in a real problem. An equivalent, simplified presentation in more traditional block diagram form is shown in Figure 1-2. In Figure 1-2, the same instantiation of hardware is represented in the block diagram for both K14(1) and K14(2), which each appear in two positions. Thus, if the hardware K14(1) fails in one of its positions, it is also a failure in the other position; likewise, the same is true for K14(2).

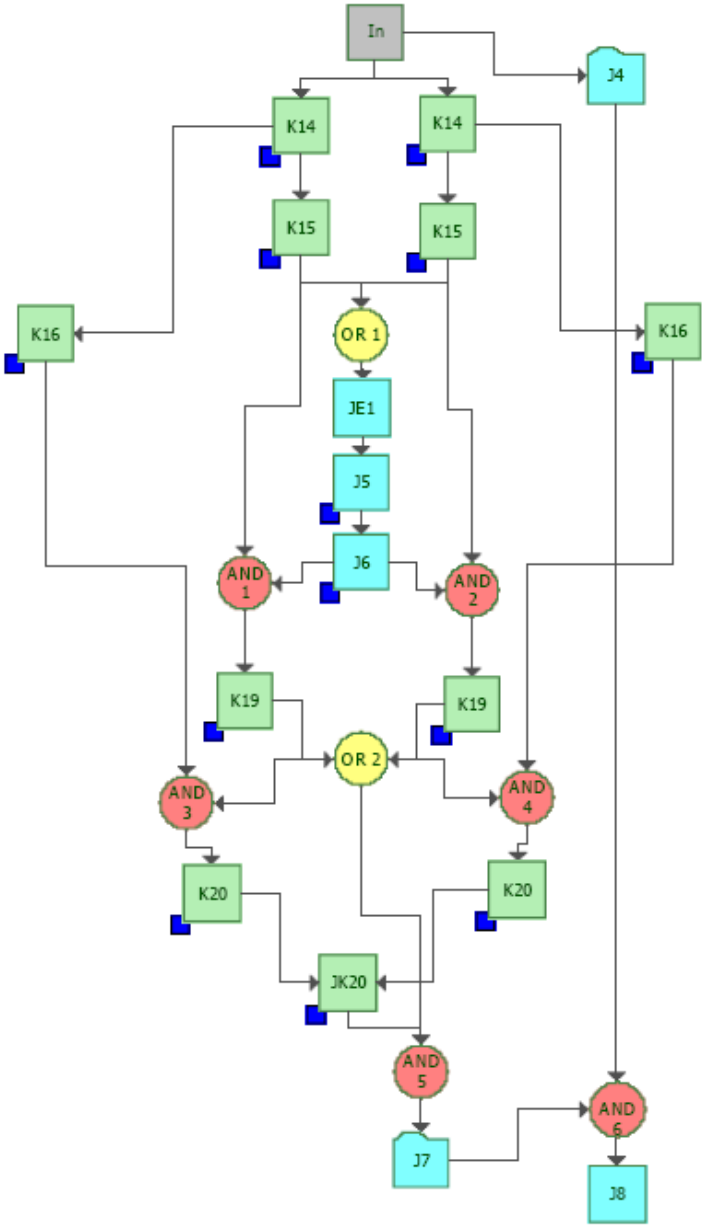

Figure 1-1. Original system model in reliability block diagram format.

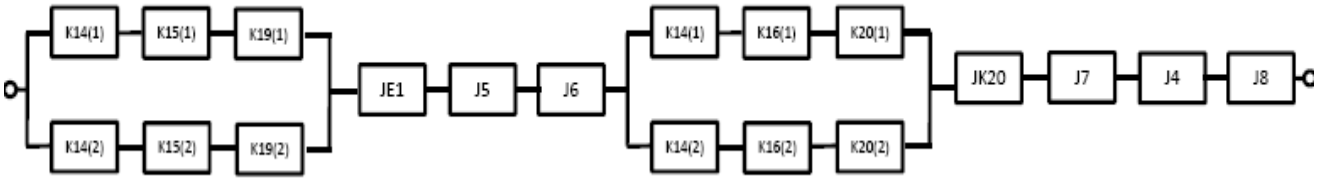

Figure 1-2. Equivalent, simplified block diagram of system model.

This results in the following equation for system reliability:

$$
\begin{aligned}
&(R_{JK20} * R_{J7} * R_{J4} * R_{J8} * R_{JE1} * R_{J5} * R_{J6})* \\
&(R_{K14(1)} * R_{K14(2)} * R_{K16(1)} * R_{K16(2)} * R_{K20(1)} * R_{K20(2)} * R_{K15(2)} * R_{K19(1)} * RK_{15(1)} * R_{K19(2)} \\
&- R_{K14(1)} * R_{K14(2)} * R_{K16(1)} * R_{K16(2)} * R_{K20(1)} * R_{K20(2)} * R_{K15(2)} * R_{K19(2)} \\
&- R_{K14(1)} * R_{K14(2)} * R_{K16(1)} * R_{K16(2)} * R_{K20(1)} * R_{K20(2)} * R_{K19(1)} * R_{K15(1)} \\
&- R_{K14(1)} * R_{K14(2)} * R_{K16(1)} * R_{K20(1)} * R_{K15(2)} * R_{K19(1)} * R_{K15(1)} * R_{K19(2)} \\
&- R_{K14(1)} * R_{K14(2)} * R_{K16(2)} * R_{K20(2)} * R_{K15(2)} * R_{K19(1)} * R_{K15(1)} * R_{K19(2)} \\
&+ R_{K14(1)} * R_{K14(2)} * R_{K16(1)} * R_{K20(1)} * R_{K15(2)} * R_{K19(2)} \\
&+ R_{K14(1)} * R_{K14(2)} * R_{K16(2)} * R_{K20(2)} * R_{K19(1)} * R_{K15(1)} \\
&+ R_{K14(1)} * R_{K16(1)} * R_{K20(1)} * R_{K19(1)} * R_{K15(1)} \\
&+ R_{K14(2)} * R_{K16(2)} * R_{K20(2)} * R_{K15(2)} * R_{K19(2)})
\end{aligned}
$$

The notation R_{JK20} denotes the probability of the JK20 event. It will be assumed that the same reliabilities apply to repeated copies of the same component. Thus $R_{K14(1)} = R_{K14(2)}$, $R_{K15(1)} = R_{K16(2)}$, $R_{K16(1)} = R_{K14(2)}$, $R_{K19(1)} = R_{K19(2)}$, $R_{K20(1)} = R_{K20(2)}$.

Example Data

We developed data sets for each of the series blocks and parallel blocks to utilize in the model. In addition, we assign a current assessment value for each event.

In the majority of cases this assessment builds on the National Nuclear Security Administration methodology for dealing with an individual component or failure mode. If X failures are seen in N tests, the failure probability assessment is typically set at X/N if X is not zero. If X is zero, failure probability assessment is typically the lesser of (1) the binomial 50% upper confidence bound (which can be shown to equal $1- 0.5^{-1/N}$) and (2) an initial predicted failure probability for that component. The logic here is that if no failures are seen, the initial estimate will be used where test quantities are limited but will jump to a lower value when we have 50-50 confidence such a value is appropriate. In a handful of cases, the current assessment does not follow this. These special cases will be discussed individually.

Event JEI

This node captures a collection of hypothesized failure modes for which we have no current data but for which we have a proposed test package. It is not time-dependent. In theory, there is both aliatory (physical) and epistemic (knowledge) uncertainty present, but we have no direct evidence on either. Unless noted otherwise, this paper will assume a reliability of 1 with no uncertainty. Chapter 3 deals with the Bayesian methodology and will illustrate ways of quantifying beliefs about these uncertainties.

Event J4

Event J4 captures the function of five components in series, J4A, J4B, J4C, J4D, and J4E, as illustrated below.

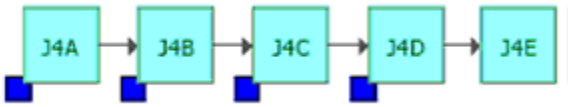

Data cannot be collected on each of the five components separately but are inferred from shared information dealing with common failure events. We can collect data directly on these failure events, but the same data may be applied to several of the J4 subevents.

J4A failure links to failure events E1, E2, E3, and E4
J4B failure also links to failure events E1, E2, E3, and E4
J4D failures links to events E1, E2, E3 (but not E4)

The following data is available on E1 through E4:

E1: 0 failures in 200,000 tests; current failure probability assessment = 0.0
E2: 0 failures in 200,000 tests, current failure probability assessment = 0.0
E3: 0 in 1,000 tests; current failure probability assessment = 0.00069
E4: 1 failure in 516 tests; the current failure probability assessment = 1/516 = 0.0019

Thus the current point-estimate reliability assessments are given as follows:

R_{J4A} = 1* 1 * (1-0.00069) * (1-0.0019) = 0.9974
R_{J4B} = 1* 1 * (1-0.00069) * (1-0.0019) = 0.9974
R_{J4D} = 1* 1 * (1-0.00069) = 0.9967

J4C and J4E are assessed (directly) from different data sources:

J4C: 1 failure in 5,000 tests; the current assessment of R_{J4C} = 0.9997
J4E: 106 successful tests, no failures; the current assessment of R_{J4E} = 1.0

In four cases, the current assessment requires some discussion. The current assessment for E3 represents the binomial 50% upper confidence limit. The current assessment for R_{J4C} does not match the expected 1/5000 = 0.0002 but is reported at 0.0003 for external (but not otherwise reported) reasons. The current reported assessment for R_{J4E} of 0.0 is less than the binomial 50% upper confidence limit, suggesting a very low initial or predicted value for the failure rate here. Chapters 2 and 3 will deal with these varied approaches to linking data to reported assessments in different ways.

Event J5

Event J5 captures the behavior of a component that has seen no failures in 3,513 tests. The currently assessed failure probability is set at the 50% upper confidence limit of 0.0002 and the best estimate of reliability, R_{J5}, is 0.9998.

Event J6

Event J6 captures the behavior of a component that has seen six failures in 31,484 tests, resulting in an assessed failure probability of 6/31,484 = 0.00019.

Event J7

Event J7 captures the function of four components in series, J7A, J7B, J7C, and J7D, as illustrated below:

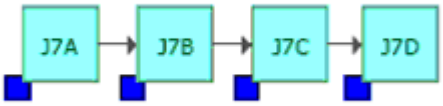

Components J7A, J7B, and J7C are tested as a unit. No failures have been seen in 2,327 tests. The current assessed unreliability is an initial predicted value of 0.0001, which is smaller than the binomial 50% upper confidence bound.

For J7D, there have been no countable failures in 71,784 countable tests (trials), which would suggest a failure probability assessment around 10^{-5}. However, since the tests involve repeated measurements on a single part, there are effectively fewer independent measures. The reported unreliability estimate is the initial failure prediction of 0.0001.

Thus, the currently assessed reliability value for J7 is $R_{J7} = (1 – 0.0001) * (1 – 0.0001) = 0.9998$.

There is a desire to move to the use of variables data as described below for J7A, J7B, and J7C.

J7A: 383 variables measurements, N(0,1). Requirement (–4.5, 4.5)
J7B: 468 variables measurements, N(0,1). Requirement (–3.8, 3.8)
J7C: 15 variables measurements, N(0,1). Requirement (–6.0, 6.0)

The shorthand “N(0,1)” means that the variables measures are distributed approximately as having Normal (Gaussian) probability distribution with mean 0 and variance 1. The shorthand “Requirement (–4.5, 4.5)” means that successful system function requires the variable be in the interval from –4.5 to 4.5.

There are 383 tests with both J7A and J7B measurements, and 85 with only the measurements of J7B.

In addition, the 2,327 pass/fail tests ensure that both J7A and J7B were within the requirements. This count includes the 468 tests described above. A compounding factor is that of the 1,859 tests that do not have data for J7A and J7B, 1,244 were done at ambient temperature and 208 were done at cold temperatures. There is no information about environmental conditions for the 468 variables tests or for the remaining 407 pass/fail tests.

The J7C observations were collected during diagnostic development and are independent of the other data.

Event J8

J8 is assessed as $R_{J8} = 1.0$ with no uncertainty.

Event JK20

Component JK20 consists of two subcomponents (C1 and C2) in parallel. The output amplitudes of the subcomponents add. Successful component function requires that the sum of the outputs be greater than some critical value k = 500,000 as measured in arbitrary output-units.

There are two independent failure modes for each subcomponent. A subcomponent may fail catastrophically, giving no output, or it may function but give less than expected output.

There are three ways that JK20 can function successfully. Figure 1-3 shows this breakout.

E1: Both C1 and C2 function, and (C1 amplitude + C2 amplitude) > *k*, where k is the required output
E2: C2 fails catastrophically, C1 functions, and C1 amplitude > *k*.
E3: C1 fails catastrophically, C2 functions, and C2 amplitude > *k*.

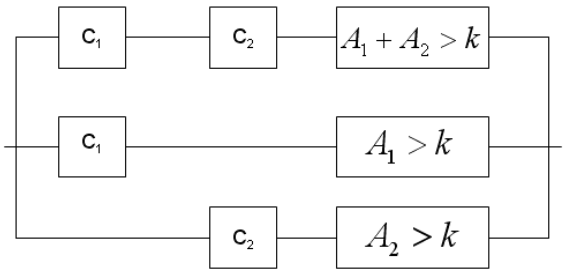

Figure 1-3. JK20 subdiagram. C1 and C2 have identical design and identical assessment data, but function independent of each other (that is, they are "mirrored").

In this figure, C_1 and C_2 represent the events that components function and A_1 and A_2 identify the output amplitudes. Events E1, E2, and E3 here represent success events. Note these are unrelated to the E1, E2, E3, and E4 used in the Event J4 discussion.

The reliability model for R_{JK20} is

$R_{JK20} = Pr(E1) + Pr(E2) + Pr(E3)$
$R_{JK20} = Pr(E1) + 2Pr(E2)$
$R_{JK20} = Pr(C_1)Pr(C_2)Pr(A_1 + A_2 > k) + 2(1 - Pr(C_1))P(C_1)P(A_1 > k)$.

There are 2500 independent tests of components of the type used for C1 and C2. Of these, 100 showed catastrophic failures. Thus, the current assessment is $Pr(C_1) = Pr(C_2) = 1 – 100/2500 = 0.96$. It is unknown whether $Pr(C_1)$ and $Pr(C_2)$ have a dependence upon time. Failure data and associated age-at-test data need to be investigated to check this. Unless otherwise specified, the sample problem assumes no dependence on time.

Component output amplitude is known to decrease as the component ages with an end of life projected at 130 years. The value *k* represents a requirement that may be exceeded until the component nears end of life. The trend in component output amplitude is assumed to follow a log-linear decrease with component age, with some unit-to-unit scatter about this trend. If y represents mean output and t represents component age, then

$Ln(y) = a + bt$.

The intercept and slope, *a* and *b*, can be estimated using linear regression on 400 available data points. One can also compute the residual standard deviation, *s*, which represents the unit-to-unit variation seen among the measured units. Separate regressions can be done (with a separate set of constants) for the cases where y_n represents the output of a single subcomponent (i.e., A_1) and where it represents the output of both subcomponents added (i.e., $A_1 + A_2$). We assume paired components are of roughly the same age. The estimation technique assumes that the standard deviation of the residuals is constant and the sample data set reflects that.

For the single and pair models, the estimated regression coefficients are summarized in Table 1-1.

Table 1-1. Regression Coefficients for Single and Pair Models.

	Regression Constants		
Regression Model	**a**	**b**	**s**
Single C1	29.22	-0.1204	0.1826
C1 and C2 Pair	29.88	-0.1204	0.1284

The single model is obtained directly from the data. The pair model was obtained by simulation, but could also have been derived analytically. The standard deviation of the residuals from the model for the pair (0.1284) agrees well with its theoretical prediction, which is the standard deviation of the residuals from the single model (0.1826) divided by the square root of 2. The intercept for the pair model is approximately ln(2) greater than the intercept for the single model, also as expected. [This theoretical prediction is obtained by expanding the function $f(y_1,y_2) =$

$\ln(e^{y1}+e^{y2})$ about $(y_1,y_2) = (0,0)$ with a first-order Taylor series approximation to estimate $\text{Var}(f(y_1,y_2))$.]

The probability that either an individual output A_1 or the summed output $A_1 + A_2$ will achieve the required amplitude is calculated by first determining the margin (K-factor) as a function of age:

$$K = (\ln(y)-\ln(k))/s,$$

and then applying the log-linear regression model for ln(y):

$$K = [\ a + bt - \ln(k)\ ] / s\ ,$$ where a, b, and s come from Table 1-1.

The probability that a particular single A_1 or the sum $A_1 + A_2$ meet the amplitude requirement is the standard normal probability ($\Pr(Z<K)$) for the appropriate single or pair version of the model coefficients.

The assessed value for R_{JK20} can then be computed from the reliability equation given with Figure 1-3, applied with time t set to the nominal end-of-life age of 130 years.

$$R_{JK20} = \Pr(C_1)\Pr(C_2)\Pr(A_1 + A_2 > k) + 2(1 - \Pr(C_1))P(C_1)P(A_1 > k).$$

The calculation is given below:

$\Pr(C_1) \sim 0.96$

$\Pr(C_2) \sim 0.96$

$\Pr(A_1 + A_2 > k) \sim P\ (Z < K_{pair}) = 1$
where, using the regression coefficients,
$K_{pair} = [(29.88 - (0.1204)(130) - 13.12)] / (0.1284) = 8.6292$

$P(A_1 > k) \sim P\ (Z < K_{single}) = 0.9929$
where, using the regression coefficients,
$K_{single} = [(29.22 - (0.1204)(130) - 13.12)] / (0.1826) = 2.4535$

Assessed $R_{JK20} \sim (0.96)^2(1) + (2)(0.04)(\ 0.96)(0.9929) = 0.9976$

Events K14, K15, K16

Events K14, K15, and K16 capture the failures of components that are not observed separately. Testing is done on an assembly made up of the these three components. Observed failures at this higher level of assembly are allocated among the three. One failure has been seen in 4,132 tests, resulting in an overall failure probability of 0.00024. This failure probability is allocated among the three failure events as follows:

K14:	(7/16)*(1/4,132)	~ 0.000106 assessed failure probability
K15:	(7/16)*(1/4,132)	~ 0.000106 assessed failure probability
K16:	(1/8)*(1/4,132)	~ 0.000029 assessed failure probability

Event K19

Event K19 captures the behavior of a component that has seen no failures in 3,338 tests. The currently estimated failure probability is assessed at the 50% upper confidence limit of 0.00021.

Event K20

Event K20 captures the behavior of a component that has seen four failures in 18,803 tests. The currently estimated failure probability is assessed at 4/18,803 = 0.000021.

2. APPROACH 1: CLASSICAL METHODOLOGY FOR PROPAGATING UNCERTAINTIES USING MOMENTS

Moment-Based Approach for Evaluating Reliability Uncertainty

This section develops the methodology for estimating potential random errors in weapon reliability estimates resulting from sampling error, based on Classical statistical theory. It also creates an approximate confidence interval for the reliability.

This section divides into several parts. It begins with some of the building blocks needed: a discussion of notation and of SNL's special handling of go/no-go test data as "adjusted binomial random variables." The third subsection reformulates the system model from Chapter 1 based on this construct and defines the system reliability estimator in terms of this reformulation. The fourth subsection develops formulas for the mean and variance of the system reliability estimator. The final subsection uses these to develop confidence intervals. Numerical results from the sample problem are presented at each relevant step.

Notations

This section adopts the following notational conventions:

Lower-case Roman letters (e.g., n, b or c) represent *known values* (like the number of tests exploring a particular failure mode).

Lower-case Greek letters (e.g., θ, τ, or μ) represent *unknown parameters* (like a "true" component failure probability). When in **boldface**, notations like $\boldsymbol{\theta}$ or $\boldsymbol{\tau}$ represent vectors of unknown parameters.

Upper-case Roman letters in italics (e.g., A or Y) represent *random variables* (i.e., quantities that in theory could take on different values according to some probability distributions). When in **boldface**, notations like $\boldsymbol{Y}$ represent vectors of random variables.

The notation $\boldsymbol{E}(Y)$ is used to denote the *expected value* of the random variable Y.

The notation $\boldsymbol{V}(Y)$ denotes the *variance* of the random variable Y.

The notations $\mathcal{R}_s(\cdot)$ and $\mathcal{R}(\cdot)$ represent the system model *functions* that roll lower-level reliability parameters into a system reliability. There are two notations because two different but equivalent forms of the function are used.

Adjusted Binomial Random Variables

Most of the data for estimating system reliability come from component- or subsystem-level go/no-go tests. SNL typically estimates the failure probability for such a component or subsystem using a random variable, *Y*, of the form

Y = X/n where X > 0 is the number of failures that have been seen in *n* relevant tests. (This is the usual maximum likelihood estimator associated with binomial random variables)

= d when no failures have been seen. Typically *d* is the minimum of some pre-assigned value, c, representing the pre-production estimate of unreliability, and $(1-0.5^{1/n})$, the binomial 50% upper confidence limit.

(1)

This form is referred to as an "adjusted binomial random variable" since it is based on a usual binomial random variable with special handling of the zero-failure case. A later section works through the properties of such a random variable.

System Model and SNL Reliability Estimator

The sample problem involves a system model of the form

$$\mathcal{R}_s(\boldsymbol{\tau}) =$$

$$\tau_{JE1}\tau_{J4A}\tau_{J4B}\tau_{J4C}\tau_{J4D}\tau_{J4E}\tau_{J5}\tau_{J6}\tau_{J7}\tau_{J8}\tau_{JK20}\sum_{j=1}^{9} b_j \tau_{14}^{c_{14,j}} \tau_{15}^{c_{15,j}} \tau_{16}^{c_{16,j}} \tau_{19}^{c_{19,j}} \tau_{20}^{c_{20,j}} \quad (2)$$

Here the τ's are parameters representing the actual but unknown reliabilities of various subsystems and components. The *b*'s are either +1 or -1. The *c*'s are integers 0, 1, or 2. The notation $\boldsymbol{\tau}$ represents the vector of all the τ's, and $\mathcal{R}_s(\boldsymbol{\tau})$ indicates the system reliability is some nonlinear function, $\mathcal{R}$, of the τ's. This is a variation on the notation used in Chapter 1. There, for instance, the notation R_{J7} was used broadly to reference either the actual failure probability or the best estimate of that value based on available data. Formal Classical handling of the problem requires making a clear notational distinction between the actual probability and the estimator. The R_{J7}-like notation will be reserved for the estimator so the new τ_{J7} has been introduced for the actual probabilities.

The system-level estimator of reliability typically used at SNL is

$$R_{SNL} =$$

$$\mathcal{R}_s(\boldsymbol{R}_{sub}) =$$

$$R_{JE1}R_{J4A}R_{J4B}R_{J4C}R_{J4D}R_{J4E}R_{J5}R_{J6}R_{J7}R_{J8}R_{JK20}\sum_{j=1}^{9} b_j R_{14}^{c_{14,j}} R_{15}^{c_{15,j}} R_{16}^{c_{16,j}} R_{19}^{c_{19,j}} R_{20}^{c_{20,j}} . \quad (3)$$

Here the *R's* are random variables estimating the unknown τ*'s*. Most of these are based on results from large numbers of go/no-go tests, although as noted in Chapter 1, R_{JK20} is more complex. The notation $\boldsymbol{R_{sub}}$ represents the vector of all the subsystem and component *R's.* Note that the system reliability estimator is the same nonlinear function, $\mathcal{R}_s$, of the *R's* as appears in the system model [Equation (2)].

While simple, R_{SNL} is not the only way one could estimate $\mathcal{R}_s(\boldsymbol{\tau})$. The Bayesian formulation, for instance, uses the system model [Equation (2)] but computes a point estimate for $\mathcal{R}_s(\boldsymbol{\tau})$ that is close to, but not identical to $\mathcal{R}_s(\boldsymbol{R_{sub}})$. Hence, it is useful to separate out the system model [Equation (2)], which may be common to many approaches, from the estimator [Equation (3)], which may not.

Rewriting System Model in Terms of Independent Data Sources

In most cases, individual *R*'s derive from adjusted binomial random variables. Table 2-1 gives the translation between the *R*'s in Equation (3) and adjusted binomial random variables Y_1 through Y_{12}. These derive directly from the discussion in Chapter 1. In some cases, more than one adjusted binomial random variable—more than one type of go/no-go test—enters into the evaluation of a given *R.* In some cases, a given adjusted binomial random applies to several *R*'s. The R_{JK20} factor has a special form involving an additional adjusted binomial random variable, Y_{JK20}, plus two other random variables derived from other data. These are discussed in the next section. Table 2-1 also gives the available data and the zero-failure values that apply in Equation (1).

A value for *d* is given in all cases. The Classical statistical formulation deals with an event space of all possible ways the data could have come out, including the event where a particular component saw no failures. The mean and variance of the *Y*'s are averages, weighted by probability, across all events in the event space. Thus, to compute the moments of *Y,* one needs the value it would take on for all points in the event space, including *d*, the zero failure case. A later section in this paper illustrates explicitly how *d* enters in to the calculations.

Folding the equations in Table 2-1 together with Equation (3), one can rewrite the reliability estimator using the following data-source parameters:

$$R_{SNL} = C_{J7} R_{JK20} \times \prod_{i=1}^{9} (1 - Y_i)^{c_i} \times \left\{ \sum_{j=1}^{9} b_j \prod_{k=10}^{12} f_{k,j}(Y_k) \right\}, \text{ where}$$

$$f_{10,j}(Y_{10}) = [(1 - \tfrac{7}{16} Y_{10})^{c_{14,j} + c_{15,j}} (1 - \tfrac{1}{8} Y_{10})^{c_{16,j}}]$$

$$f_{11,j}(Y_{11}) = (1 - Y_{11})^{c_{19,j}}$$

$$f_{12,j}(Y_{12}) = (1 - Y_{12})^{c_{20},j}. \qquad (4)$$

The *b*'s and *c*'s are constants, as shown in Table 2-2.

Equation (4) illustrates that R_{SNL} can be viewed as the product of factors involving independent variables, including one factor, shown in brackets, that consists of a sum-product that collects the contribution of components that appear in parallel.

Table 2-1. Assessed Reliability Factors and Adjusted Binomial Random Variables.

Model Reliability Factor	Adjusted Bino-mial RV	# Failures (*X*)	# Tests (*n*)	Zero Failure Value (d)	Current Assessed Value for Y	Note
$R_{JE1} = 1$ *(with no uncertainty)*					0	(1)
$R_{J4A} = (1- Y_1) (1- Y_2) (1- Y_3) (1-Y_4)$	Y_1	0	200,000	0	0	(2)
$R_{J4B} = (1- Y_1) (1- Y_2) (1- Y_3) (1-Y_4)$	Y_2	0	200,000	0	0	(2)
$R_{J4D} = (1- Y_1) (1- Y_2) (1- Y_3)$	Y_3	0	1,000	0.00069	0.00069	(3)
	Y_4	1	516	0.0013	0.0019	(4)
$R_{J4C}= (1-Y_5)$	Y_5	1	5,000	0.0003	0.0002	(5)
$R_{J4E}= (1-Y_6)$	Y_6	0	106	0	0	(2)
$R_{J5}= (1-Y_7)$	Y_7	0	3,513	0.00020	0.00020	(3)
$R_{J6}= (1-Y_8)$	Y_8	6	31,484	0.000022	0.00019	(4)
$R_{J7} = (1-Y_9)\ C_{J7}$ $C_{J7} = 0.9999$ is a constant. (71,784 data treated as not applicable.)	Y_9	0	2,327	0.0001	0.0001	(2)
$R_{J8} = 1$ (with no uncertainty)					0	(1)
$R_{K14}= (1 - (7/16)Y_{10})$ $R_{K15} = (1 - (7/16)Y_{10})$ $R_{K16} = (1 - (1/8)Y_{10})$	Y_{10}	1	4,132	0.00017	0.0024	(4)
$R_{K19}= (1-Y_{11})$	Y_{11}	0	3,338	0.00021	0.00021	(3)
$R_{K20}= (1-Y_{12})$	Y_{12}	4	18,803	0.000037	0.00021	(4)
$R_{JK20} = 2P_1(Y_{JK20})(1-Y_{JK20}) + P_2(1-Y_{JK20})^2$ P_1 and P_2 are derived from regression P_1 = Prob (sufficient output from 1) P_2 = Prob (sufficient output from 2)	Y_{JK20}	100 (400 obs. on output vs. age)	2500	0.00028	0.04	(4) (6)

Data sources as described in Chapter 1.

Notes: (1) Omitted from subsequent calculation.

(2) d is the initial prediction value, which is used as the current assessed failure probability.

(3) d is the 50% upper confidence limit, which is used as the current assessed failure probability.

(4) The currently assessed unreliability is X/n. No zero-failure value was given or could be inferred in the sample problem. It could be either 50% upper confidence limit or some initial predicted value. Without specific information about an initial predicted value, the zero-failure value, d, is set to the 50% upper confidence bound.

(5) Even with one failure, the reported unreliability for this event in the sample problem is not X/n. Presumably, the reported unreliability represents a prediction that was not replaced when failures were seen. This analysis uses X/n as the currently assessed unreliability. The table value of d is set to the reported (predicted?) unreliability.

(6) Involves continuous measurement data (see JK20 component description).

Table 2-2. Model Constants.

	b_j
j=1	1
j=2	-1
j=3	-1
j=4	-1
j=5	-1
j=6	1
j=7	1
j=8	1
j=9	1

	$c_{14,j}$	$c_{15,j}$	$c_{16,j}$	$c_{19,j}$	$c_{20,j}$
j=1	2	2	2	2	2
j=2	2	1	2	1	2
j=3	2	1	2	1	2
j=4	2	2	1	2	1
j=5	2	2	1	2	1
j=6	2	1	1	1	1
j=7	2	1	1	1	1
j=8	1	1	1	1	1
j=9	1	1	1	1	1

c_1=3
c_2=3
c_3=3
c_4=2
c_5=1
c_6=1
c_7=1
c_8=1
c_9=1

JK20 Component Model

The R_{JK20} factor in Equation (3) is more complicated than the others. The following section recasts the model presented in Chapter 1 to illustrate that R_{JK20} can be written as a nonlinear function of three independent random variables. From Chapter 1,

$R_{JK20} = 2P_1 Y_{JK20} (1-Y_{JK20}) + P_2 (1-Y_{JK20})^2$, where

P_1 estimates the probability one component at end of life gives output above threshold k,
P_2 estimates the probability two components at end of life sum to give output above threshold k. (5)

P_1 and P_2 derive from component test data of output versus time. Again, following Chapter 1, if $A_1(t)$ represents the output from one component at time t, the following log-linear model applies

$ln(A_1(t)) = a + \beta t + E_1$,

where E_1 is a Gaussian random variable with mean 0 and variance σ^2. (6)

This follows the discussion in Chapter 1, with some changes of notation to follow the conventions in this chapter. The parameters α, β, and σ^2 are not known, but can be estimated via standard linear least squares regression estimators from the 400 $(A_1(t), t)$ pairs provided in the sample problem. Let the estimators be denoted A, B, and S^2. (This follows this chapter's notational conventions; Chapter 1 used lower case a, b, and s.) The mean log output at time t is

$\mu = \alpha + \beta t$, (7)

which can be estimated by

$$M = A + Bt. \tag{8}$$

M will be evaluated at the end of life of t = 130.

Since E_1 in Equation (6) is assumed to have a Gaussian distribution, the calculation for P_1 is then

$$P_1 = \Phi((M - \ln(k)) / S), \tag{9}$$

where Φ is the Gaussian cumulative. Note that P_1, as a function of two other random variables, M and S, is itself a random variable. Also note that under the model in Equation (6), the usual regression estimators, M and S, are independent.

One can also show that the probability that the sum of two components' outputs is *k* or greater can be approximated by

$$P_2 = \Phi(\sqrt{2}(M + \ln(2) - \ln k)) / S). \tag{10}$$

Putting this all together, R_{JK20} is thus the following nonlinear function of the three independent random variables Y_{JK20}, M, and S:

$$R_{JK20} =$$

$$= 2\Phi((M - \ln(y_r)) / S)\left[Y_{JK20}(1 - Y_{JK20})\right] + \Phi(\sqrt{2}(M + \ln(2) - \ln(y_r)) / S)\left[(1 - Y_{JK20})^2\right] \tag{11}$$

Summary Notations for Subsystem and Data-Source Representations

Equation (4) provides an equivalent system model to Equation (3) with vector of subsystem random variables, $\boldsymbol{R_{sub}}$, replaced by the vector of independent random variables linked to data sources. With a small abuse of notation, let

$\boldsymbol{Y} = (Y_1, Y_2, \ldots Y_{12}, Y_{JK20}, M, S)$ and

$$R_{SNL} = \mathcal{R}_s(\boldsymbol{R_{sub}}) = \mathcal{R}(\boldsymbol{Y}). \tag{12}$$

The full form of $\mathcal{R}$ combines Equation (4) with Equation (11):

$$R_{SNL} = \mathcal{R}(\boldsymbol{Y})$$

$$= C_{J7} \times \left\{2\Phi((M - \ln(k)) / S)\left[Y_{JK20}(1 - Y_{JK20})\right] + \Phi(\sqrt{2}(M + \ln(2) - \ln(k)) / S)\left[(1 - Y_{JK20})^2\right]\right\} \times \prod_{i=1}^{9}(1 - Y_i)^{c_i} \times \left\{\sum_{j=1}^{9} b_j \prod_{k=10}^{12} f_{k,j}(Y_k)\right\},$$

where

$$f_{10,j}(Y_{10}) = [(1-\tfrac{7}{16}Y_{10})^{c_{14,j}+c_{15,j}}(1-\tfrac{1}{8}Y_{10})^{c_{16,i}j}],$$

$$f_{11,j}(Y_{11}) = (1-Y_{11})^{c_{19,j}},$$
$$f_{12,j}(Y_{12}) = (1-Y_{12})^{c_{20},j},$$

and the *b*'s and *c*'s are as in Table 2-2. (13)

The same equivalence applies to the theoretical model involving unknown parameters. Each Y_i estimates some probability θ_i. The regression random variables M and S^2 estimate parameters μ and σ^2. Thus, with similar notation as before, let $\boldsymbol{\theta} = (\theta_1, \theta_2, \ldots, \theta_{12}, \theta_{JK20}, \mu, \sigma^2)$. Then, for the same $\mathcal{R}_s$ and $\mathcal{R}$ as above,

$$\mathcal{R}_s(\boldsymbol{\tau}) = \mathcal{R}(\boldsymbol{\theta})$$

$$= C_{J7} \times \left\{2\Phi((\mu - \ln(k))/\sigma)\left[\pi_{JK20}(1-\theta_{JK20})\right] + \Phi(\sqrt{2}(\mu + \ln(2) - \ln(k))/\sigma)\left[(1-\theta_{JK20})^2\right]\right\} \times \prod_{i=1}^{9}(1-\theta)^{c_i} \times \left\{\sum_{j=1}^{9} b_j \prod_{k=10}^{12} f_{k,j}(\theta_k)\right\}. \quad (14)$$

Because it involves independent random variables, the formulation involving $\mathcal{R}(Y)$ is easier to use as the basis for constructing confidence statements. Working with $\mathcal{R}_s(\boldsymbol{R}_{sub})$ requires tracking the correlations between the component or subsystem reliability estimators in $\boldsymbol{R}_{sub}$ introduced because some rely in part on the same test data. Note, however, that the restructuring from $\mathcal{R}_s(\boldsymbol{R}_{sub})$ – a structure based on the reliability block diagram and system operation – to $\mathcal{R}(Y)$ – a structure based on independent data sources – may take significant effort. It is possible that the $\mathcal{R}(Y)$ model may be considerably larger than the $\mathcal{R}_s(\boldsymbol{R}_{sub})$ for some systems. This could happen, for instance, if many independent data subsets are applied in more complex ways than was the case for the J4 event here.

Estimating the Mean and Variance of R_{SNL}

The mean and variance of R_{SNL} can be approximated from moments of the random variables entering into it, Y_1 through Y_{12}, Y_{JK20}, and the regression estimates *M* and *S*. This mean and variance are used to develop confidence intervals for $\mathcal{R}(\boldsymbol{\theta})$.

General Formulas for the Mean and Variance of a Function of Random Variables

Two general approximation formulas are used extensively:

$$\boldsymbol{E}(f(Y)) \approx f(\boldsymbol{E}(Y)) + f''(\boldsymbol{E}(Y))Var(Y)/2$$

$$\boldsymbol{V}\left[f(Y_1, Y_2, Y_3, ...)\right] \approx \left[\frac{\partial f}{\partial Y_1}\right]^2 \boldsymbol{V}(Y_1) + \left[\frac{\partial f}{\partial Y_2}\right]^2 \boldsymbol{V}(Y_2) + \left[\frac{\partial f}{\partial Y_3}\right]^2 \boldsymbol{V}(Y_3) + ...$$

where Y, Y_1, Y_2, … are independent univariate random variables (15)

To see the first, let $\mu = \boldsymbol{E}(Y)$, write $f(Y) \sim f(\mu) + f'(\mu))(Y - \mu) + f''(\mu)(Y-\mu)^2/2$, and take expected values on both sides. In some cases where it appears the second term is quite small, only the first term is used.

A multivariate version of the same leads to the familiar variance expansion.[†]

Mean and Variance for Adjusted Binomial Random Variables

Random variables Y_1 through Y_{12} and Y_{JK20} have adjusted binomial distributions of the form given in Equation (1). Following the notation in Equation (1), if X has a binomial distribution associated with n trials and probability of failure θ, then the probability that random variable X (upper case) takes some particular numerical value x (lower case) is given by

$$\Pr(X = x) = \binom{n}{x}\theta^x(1-\theta)^{n-x}, \text{ for } x = 0, 1, \ldots n, \text{ where } \binom{n}{x} = \frac{n!}{(n-x)!x!} \quad (16)$$

The adjusted binomial random variable follows the same functional formexcept for special handling of the zero-failure case:

$$\Pr(Y = d) = (1-\theta)^n, \text{ and}$$

$$\Pr(Y = x/n) = \binom{n}{x}\theta^x(1-\theta)^{n-x} \quad \text{for x = 1, 2, ..., n.} \quad (17)$$

[†] This is standard practice. See, for example, Taylor and Kuyatt (1994).

From this, the moments of an adjusted binomial random variable are easily computed. For the mean:

$$\boldsymbol{E}(Y) = \theta + (1-\theta)^n d \quad = \text{value for regular binomial + "new" zero failure term.} \tag{18}$$

Note that even though Y was constructed to provide an estimate of θ, it is a biased (in the statistical sense) estimate: $\boldsymbol{E}(\mathrm{Y}) \neq \theta$.

For the variance:

$$\boldsymbol{V}(Y) = \boldsymbol{E}(Y^2) - [\boldsymbol{E}(Y)]^2 \text{ and}$$

$$\boldsymbol{E}(Y^2) = [\theta(1-\theta)/n + \theta^2] + d^2(1-\theta)^n \quad = \text{value for regular binomial + "new" } X = 0 \text{ term, so}$$

$$\boldsymbol{V}(Y) = \theta(1-\theta)/n + (d-2\theta)d(1-\theta)^n - d^2(1-\theta)^{2n}. \tag{19}$$

Equations (18) and (19) involve two known parameters, n and d, and one unknown parameter, θ. Thus, these equations cannot be used directly to give a numerical estimate of moments. A natural way to approximate $\boldsymbol{E}(Y)$ *and* $\boldsymbol{V}(Y)$ would be to replace θ by the realized value of the Y in question. If there were no failures, that would be the d value shown in Table 2-1. If there were failures, that would be the X/n from Table 2-1.

Mean and Variance for Individual Model Factors

To compute the mean and variance of R_{SNL} in Equation (13), one needs the mean and variance of each of the factors. Factors are of four forms:

C_{J7}	= a constant.
R_{JK20}	= as expanded in Equation (11).
$(1-Y_i)^{ci}$	= for i = 1, 2, …, 9 and the Y_i's being adjusted binomial random variables.
$\left\{\sum_{j=1}^{9} b_j \prod_{k=10}^{12} f_{k,j}(Y_k)\right\}$	= the sum-product term.

As a constant, C_{J7} essentially has mean C_{J7} and variance 0.

The moments of R_{JK20} can be estimated by applying the general formulas [Equation (15)] to the full equation for R_{JK20} given in Equation (11). For the mean, only the first term in Equation (15) is used. The numerical estimate of the mean is then just Equation (11) with the random variables M and S replaced by their observed values and the adjusted binomial random variable Y_{JK20} replaced by a numerical estimate of its expected value, $Y_{JK20} + d(1- Y_{JK20})^n$.

Likewise, the variance computation follows Equation (15):

$$\boldsymbol{V}\left[R_{JK20}\right] \approx \left(\frac{\partial_{RJK20}}{\partial Y_{JK20}}\right)^2 \boldsymbol{V}(Y_{JK20}) + \left(\frac{\partial_{RJK20}}{\partial M}\right)^2 \boldsymbol{V}(M) + \left(\frac{\partial_{RJK20}}{\partial S^2}\right)^2 \boldsymbol{V}(S^2). \tag{20}$$

Here the partial derivatives are evaluated at the expected values for the variables. The calculations are straightforward if messy. Note they require $\Phi'(x) = \frac{1}{\sqrt{2\pi}} e^{-x^2/2}$. A numerical result is obtained by the same sort of replacements as were done for the mean. Unknown parameters $\mu = \boldsymbol{E}(M)$ and $\sigma^2 = \boldsymbol{E}(S^2)$ are replaced by the observed values for *M* and *S*. $\boldsymbol{E}(Y_{JK20})$ is replaced by $Y_{JK20} + d(1- Y_{JK20})^n$. The variances in Equation (20) come from various sources. $\boldsymbol{V}(Y_{JK20})$ can be estimated using Equation (19) with θ replaced by the observed value of $Y_{JK20.}$ $\boldsymbol{V}(M)$ can be estimated using from the usual linear regression analysis. (For the t set to the end-of-life age of 130 years, the regression on the 400-point data set gives $\boldsymbol{V}(M)$ = 0.05503. This corresponds to a standard error for M — the square root of $\boldsymbol{V}(M)$ – equal to 0.2346.) $\boldsymbol{V}(S^2)$ is typically not computed as part of the usual regression analysis, but can be derived using the same theory. Under the usual linear regression model, S^2 is distributed as a multiple of a Chi-Square distribution, $S^2 \sim \sigma^2 \chi_\nu^2 / \nu$, for some number of degrees of freedom ν. Here, ν = 398. Hence,

$$\boldsymbol{V}(S^2) = 2\sigma^4/\nu \quad \sim 2S^4/398.$$

For factors of the form $(1-Y)^c$, the approximation formula Equation (15) gives

$$\boldsymbol{E}((1-Y)^c) \approx (1-\boldsymbol{E}(Y))^c + \tfrac{1}{2}c(c-1)(1-\boldsymbol{E}(Y))^{c-2}\boldsymbol{V}(Y) \text{ and}$$

$$\boldsymbol{V}\left[(1-Y)^c\right] \approx \left[c(1-E(Y))^{c-1}\right]^2 \boldsymbol{V}(Y). \tag{21}$$

As before, numerical estimates can be obtained by using Equations (18) and (19) for $\boldsymbol{E}(Y)$ and $\boldsymbol{V}(Y)$, respectively, with the unknown parameter θ replaced by the observed value for the *Y* in question.

For the sum-product term,

$$\boldsymbol{E}\left[\sum_{j=1}^{9} b_j \prod_{k=10}^{12} f_{k,j}(Y_k)\right] \quad \approx \sum_{j=1}^{9} b_j \prod_{k=10}^{12} f_{k,j}(\boldsymbol{E}[Y_k]) \quad \text{and}$$

$$\boldsymbol{V}\left[\sum_{j=1}^{9} b_j \prod_{k=10}^{12} f_{k,j}(Y_k)\right] \approx \sum_{i=10}^{12} \left\{\frac{\partial}{\partial Y_i}\left[\sum_{j=1}^{9} b_j \prod_{k=10}^{12} f_{k,j}(Y_k)\right]\right\}^2 \boldsymbol{V}(Y_i). \tag{22}$$

The derivatives—straightforward if messy—are evaluated at the means of the random variables. As before, numerical estimates can be obtained by using formulas 18 and 19 with unknown θ's replaced by observed *Y*'s.

Mean and Variance for Product of Model Factors

The last step is then to compute the mean and variance of R_{SNL} given the moments of each of the factors. For products, the approximation formulas [Equation (15)] take on some simple forms.

Suppose A_i are independent random variables for i = 1, 2, …, then

$$\boldsymbol{E}\left[\prod_i A_i\right] = \prod_i \boldsymbol{E}(A_i)$$

$$\boldsymbol{v}\left[\prod_i A_i\right] \approx \sum_i \frac{\boldsymbol{V}(A_i)\left[\prod_i \boldsymbol{E}^2(A_i)\right]}{\boldsymbol{E}^2(A_i)}. \qquad (23)$$

The latter gives the variance of the product as the sum of variance contributions associated with each factor.

Numerical Results

Table 2-3 gives numerical results of the computations described above, broken up by model factor. The calculations are for an R_{JK20} end-of-life value of t = 130 years.

Table 2-3. R_{SNL} Computation by Factor, t = 130 Years.

Model Factor	Estimated Value for Factor	1-Estimate	Fraction of unreliability	Expected value: E (Factor)	Variance: V (Factor)	Variance contribution to product: $E^2(R)$* (Var(F)/E^2(F))	Fraction of variance
C_{J7}	0.9999	0.0001	1%	0.9999	0	0	0%
R_{JK20}	0.9978	0.0022	24%	0.9978	4.13E-06	4.06E-06	25%
$(1-Y_1)^3$	1.0000	0.0000	0%	1.0000	0	0	0%
$(1-Y_2)^3$	1.0000	0.0000	0%	1.0000	0	0	0%
$(1-Y_3)^3$	0.9979	0.0021	23%	0.9969	2.97E-06	2.92E-06	18%
$(1-Y_4)^2$	0.9961	0.0039	44%	0.9952	9.11E-06	9.00E-06	56%
$(1-Y_5)$	0.9998	0.0002	2%	0.9997	2.41E-08	2.35E-08	0%
$(1-Y_6)$	1.0000	0.0000	0%	1.0000	0	0	0%
$(1-Y_7)$	0.9998	0.0002	2%	0.9997	2.70E-08	2.64E-08	0%
$(1-Y_8)$	0.9998	0.0002	2%	0.9998	6.03E-09	5.90E-09	0%
$(1-Y_9)$	0.9999	0.0001	1%	0.9998	2.88E-08	2.81E-08	0%
Sumproduct	1.0000	0.0000	0%	1.0000	1.92E-13	1.88E-13	0%
	Est for R_{SNL}	**Est for $(1-R_{SNL})$**		**$E(R_{SNL})$**		**$Var(R_{SNL})$**	
	0.9911	**0.0089**		**0.9889**		**1.6064E-05**	
	(product)			**(product)**		**(sum)**	

The row labeled "Sumproduct" evaluates $\sum_{j=1}^{9} b_j \prod_{k=10}^{12} f_{k,j}(Y_k)$ with random variables Y_{10}, Y_{11}, and Y_{12}.

Note that the R_{JK20}, Y_3, and Y_4 factors are the only factors that contribute substantially to system unreliability. The "Fraction of variance" column indicates the largest contributors to uncertainty. Not too surprisingly, the largest contributors to unreliability are the largest contributors to uncertainty, although the numerical values are not identical.

Interval Estimates for System Reliability

Based on the moments of $R_{SNL,}$ one can generate an interval estimate, bounds p_L and p_U, that, with some confidence, encompasses the value of $\mathcal{R}(\theta)$, the true but unknown reliability. To do that, one needs a distributional form for R_{SNL}. As a nonlinear function of adjusted binomials, the Gaussian random variable M, and the Chi-square random variable S^2, R_{SNL} does not have a simple distributional form. This analysis uses a common approximation—cited in Diegert (2006), for instance—of assuming that it has binomial distribution with some equivalent number of tests. That is, this analysis associates R_{SNL} with a binomial random variable $R_{EQ} = X_{EQ}/n_{eq}$, where X_{EQ} equivalent failures are observed in n_{eq} tests, and then builds an approximate binomial confidence interval based on R_{EQ}. This provides a means of getting a reasonable distributional shape for R_{SNL}, but specific meaning should not be applied to the exact values of X_{EQ} and n_{eq}.

The choice of X_{EQ} is complicated by R_{SNL} being a biased estimator of system failure probability, $\mathcal{R}(\theta)$. If R_{EQ} is to be used to build confidence intervals $\mathcal{R}(\theta)$, one would like

$\boldsymbol{E}(R_{EQ}) = \mathcal{R}(\theta)$ or, equivalently

$$\boldsymbol{E}(X_{EQ}) = \mathcal{R}(\theta) \times n_{eq}. \tag{24}$$

(For the moment, assume n_{eq} is known. It is discussed below.) To develop this, define

$$Bias(R_{SNL}) = \boldsymbol{E}(R_{SNL}) - \mathcal{R}(\theta). \tag{25}$$

Note that all of these depend on unknown parameters. Putting Equation (24) and Equation (25) together and rearranging gives

$$\boldsymbol{E}(X_{EQ}) = [\boldsymbol{E}(R_{SNL}) - Bias(R_{SNL})] \times n_{eq.} \tag{26}$$

This then suggests the association

$$X_{EQ} \sim [R_{SNL} - Bias(R_{SNL})] \times n_{eq,} \tag{27}$$

provided one can develop a numerical estimate of $Bias(R_{SNL})$. There are two ways to do so.

First, and very simply, if the calculation of R_{SNL} is carried out with regular binomial random variables rather than adjusted binomial random variables (i.e., if no failures are observed for a component, assess the reliability as 1), the resulting estimator, call it R_{BIN}, has only small bias. (That small bias occurs because system reliability is a nonlinear function of the component and subsystem reliabilities. Informal numerical studies indicate that bias—as partially measured by the second derivative term in Equation (15)—is small compared to that introduced by using adjusted binomial random variables. However, there has been no full examination of the residual bias.)

Thus,

$$Bias(R_{SNL}) \text{ Estimate \#1} = R_{SNL} - R_{BIN.} \tag{28}$$

A second approach makes use of the *computed* value for $\boldsymbol{E}(R_{SNL.})$. To introduce this, some additional notation is needed. One can write the theoretical value for $\boldsymbol{E}(R_{SNL})$ as some function, $\mathcal{E}(\theta)$, of the various unknown parameters. We can write the *computed* value for $\boldsymbol{E}(R_{SNL})$ as the same function $\mathcal{E}(\boldsymbol{Y})$ applied to the estimated failure probabilities $Y = (Y_1, Y_2, \ldots Y_{12}, Y_{JK20}, M, S^2)$. With this notation, Equation (25) can be rewritten:

$$Bias(R_{SNL}) = \boldsymbol{E}(R_{SNL}) - \mathcal{R}(\boldsymbol{\theta}) = \mathcal{E}(\boldsymbol{\theta}) - \mathcal{R}(\boldsymbol{\theta}),$$

which suggests

$$\text{Bias Estimate \#2} \sim \mathcal{E}(\boldsymbol{Y}) - \mathcal{R}(\boldsymbol{Y})$$

$$= \text{numerical estimate for } \boldsymbol{E}(R_{SNL}) - R_{SNL}. \tag{29}$$

This works provided that the inaccuracy in moving from $\mathcal{E}(\boldsymbol{\theta})$ to $\mathcal{E}(\boldsymbol{Y})$ is the same as that in moving from $\mathcal{R}(\boldsymbol{\theta})$ to $\mathcal{R}(\boldsymbol{Y})$. That appears to be a reasonable approximation, but as was the case with bias estimate #1, there has been no formal examination of this approximation's properties. For the sample problem,

Bias Estimate #1 = –0.0023
Bias Estimate #2 = –0.0022.

These are reassuringly close. In the following, bias estimate #2 is used.

The value of n_{eq} can be developed from the formulas for the mean and variance of a binomial random variable:

$$\boldsymbol{E}(R_{EQ}) \sim p_{equiv}$$
$$\boldsymbol{V}(R_{EQ}) \sim p_{equiv}(1-p_{equiv})/n_{eq}$$

Solving:

$$n_{eq} \sim (\boldsymbol{E}(R_{EQ}))(1-\boldsymbol{E}(R_{EQ}))/\boldsymbol{V}(R_{EQ}). \quad (30)$$

It is natural to replaces $\boldsymbol{V}(R_{EQ})$ with its estimated value for the variance of R_{SNL} (1.61×10^{-5} in Table 2-3). Although the discussion above indicates that there are many considerations in associating a numerical value with $\boldsymbol{E}(R_{EQ})$, it seems most natural that $\boldsymbol{E}(R_{EQ})$ should be evaluated in the same way as $\boldsymbol{V}(R_{EQ})$, with estimated value (0.9889) in Table 2-3.

In the computational example, one obtains n_{eq} = 681.1. Then applying Equation (28) with bias estimate #2, one gets X_{eq} = 676.6. (These calculations were done to full precision and then rounded, rather than using rounded values throughout.)

Approximate *100(1-α)* confidence intervals of the form (p_L, p_U) can be found by solving the equations

$$\sum_{j=X}^{N}\binom{N}{j}(p_L)^j(1-p_L)^{N-j} = \alpha/2 \quad \text{and} \quad \sum_{j=0}^{X}\binom{N}{j}(p_U)^j(1-p_U)^{N-j} = \alpha/2. \quad (31)$$

The limits p_L and p_U can be evaluated via reference to the incomplete beta function.‡ In EXCEL, the calls are p_L = BETAINV(α/2, X, N-X+1) and p_U = BETAINV(1-α/2, X+1, N-X).

In this context, p_L is referred to as the lower *100(α/2)*% confidence limit, and p_U is the upper *100(1-α/2)*% confidence limit. For example, for a 90% confidence interval, p_L is the lower 5% confidence limit, and p_U is the upper 95% limit.

In the sample problem, a 90% confidence interval is given as (0.9855, 0.9975), with, again, R_{SNL} = 0.9911. A 95% interval is given by (0.9839, 0.9980).

Calculation with J4E Adjustment

A variation on the calculation above was done to explore the sensitivity to the handling of the J4E event. In the calculation above, the reliability of this event was set to 1 based on no observed failures in 106 tests and, implicitly, a strong initial belief that the failure probability was very low. This shown in Table 2-1, where the zero-failure value (d) for Y_6 is set to 0, as is the failure assessment ($1-Y_6$). In this variation, the zero-failure value for Y_6. is changed to d = 0.00652, which is the lower 50% binomial confidence limit with 106 tests. The calculational formulas are otherwise the same.

‡ See Chapter 3, Section 7.2 of Johnson and Kotz (1969).

A few results are as follows:

$R_{SNL} = 0.9847$
$E(R_{SNL}) \sim 0.9793$
$Var(R_{SNL}) \sim 4.4335 \times 10^{-5}$
Bias Estimate #2 = –0.0054
$n_{eq} = 457.9$
$X_{eq} = 453.4$
90% confidence interval: (0.9785, 0.9963)
95% confidence interval: (0.9761, 0.9970)

3. APPROACH 2: BAYESIAN METHODOLOGY FOR PROPAGATING UNCERTAINTIES

Reliability Block Diagram

We now demonstrate the Bayesian methodology on the same system given in the block diagram of Figure 3-1 (a repeat of Figure 1-2).

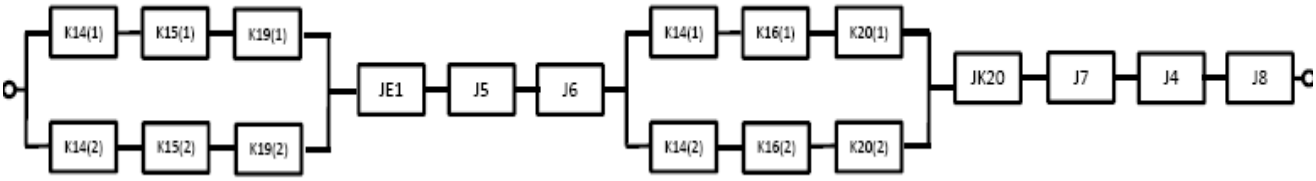

Figure 3-1. Reliability block diagram for the sample system.

Each block represents a component within the system. We use the term component more generally than is traditionally done in the reliability literature. A component here can represent a subsystem. Blocks beginning with the letter "K" are generally in parallel, whereas blocks beginning with "J" represent series systems. For example, block J4 is a subsystem consisting of components J4A, J4B, J4C, and J4D in series. In fact, we could replace block J4 in Figure 3-1 with a series of four blocks labeled J4A–J4D. Identical but multiple components are distinguished with a number after them as in K14(1) and K14(2), which are two parts of the same type in parallel.

The reliability block diagram is equivalent to the one presented in Figure 1-1, which is produced by ReliaSoft software in use by SNL. These diagrams are equivalent and lead to the system reliability equation:

$$
\begin{aligned}
&(R_{JK20} * R_{J7} * R_{J4} * R_{J8} * R_{JE1} * R_{J5} * R_{J6}) * \\
&(R_{K14(1)} * R_{K14(2)} * R_{K16(1)} * R_{K16(2)} * R_{K20(1)} * R_{K20(2)} * R_{K15(2)} * R_{K19(1)} * RK_{15(1)} * R_{K19(2)} \\
&- R_{K14(1)} * R_{K14(2)} * R_{K16(1)} * R_{K16(2)} * R_{K20(1)} * R_{K20(2)} * R_{K15(2)} * R_{K19(2)} \\
&- R_{K14(1)} * R_{K14(2)} * R_{K16(1)} * R_{K16(2)} * R_{K20(1)} * R_{K20(2)} * R_{K19(1)} * R_{K15(1)} \\
&- R_{K14(1)} * R_{K14(2)} * R_{K16(1)} * R_{K20(1)} * R_{K15(2)} * R_{K19(1)} * R_{K15(1)} * R_{K19(2)} \\
&- R_{K14(1)} * R_{K14(2)} * R_{K16(2)} * R_{K20(2)} * R_{K15(2)} * R_{K19(1)} * R_{K15(1)} * R_{K19(2)} \\
&+ R_{K14(1)} * R_{K14(2)} * R_{K16(1)} * R_{K20(1)} * R_{K15(2)} * R_{K19(2)} \\
&+ R_{K14(1)} * R_{K14(2)} * R_{K16(2)} * R_{K20(2)} * R_{K19(1)} * R_{K15(1)} \\
&+ R_{K14(1)} * R_{K16(1)} * R_{K20(1)} * R_{K19(1)} * R_{K15(1)} \\
&+ R_{K14(2)} * R_{K16(2)} * R_{K20(2)} * R_{K15(2)} * R_{K19(2)}) \qquad (32)
\end{aligned}
$$

In Equation (33), the notation $R_{(.)}$ represents the reliability of component (.), and R_{SYS} is the overall system reliability for the block diagram of Figure 3-1. We assume that multiple parts of the same type (e.g., K14(1) and K14(2)) are identical but different parts and have the same

reliability distribution. Chapter 1 details component definitions and data for the model. For more details on the methodology described in this section, see Huzurbazar et al (2009).

Overview of Bayesian Reliability Methodology

To estimate the system reliability of Equation (34), we estimate the component reliability of each component (J4, J5,…, JK20) individually. We use a Bayesian inference approach (Berger 1993; Gelman et al. 1995) where a prior for each component is specified and available data is combined with the prior to obtain a posterior distribution.

Bayesian inference provides a mechanism for making inferences about unknown parameters in a model, updating our knowledge of the mechanism that generated the data, and ultimately making predictions, with associated uncertainty, about system reliability.

The basic terminology used in Bayesian inference includes the terms prior distribution, posterior distribution, likelihood function, and predictive distribution. Let θ represent the parameter vector and let $f(x|\theta)$ represent the probability density function or model of one observation. The prior distribution, $\pi(\theta)$, describes a priori beliefs about the plausibility of the model. For n observations $X_1 \ldots X_n$, the likelihood function is defined by

$$L(\theta \mid x_1,...,x_n) = f_{X_1,...,X_n}(x_1,...,x_n \mid \theta),$$

where the right side is the joint distribution of the data. Our prior belief about θ is updated by using the data through the likelihood function. This updated belief is represented by the posterior probability distribution on θ denoted by $\pi(\theta|x)$ and calculated by

$$\pi(\theta \mid x_1,...,x_n) \propto L(\theta \mid x_1,...,x_n)\pi(\theta).$$

The Bayes predictive density of a future observation Z given data *D* is

$$f(z \mid D) = \int f(z,\theta \mid D)d\theta = \int f(z \mid \theta)\pi(\theta \mid D)d\theta$$

where θ represents the parameter vector and π is the posterior distribution of θ.

Depending on the complexity of the distributional forms, we either obtain an analytical closed-form posterior or an approximation based on sampling from the integral form of the posterior using MCMC. We provide both a point estimate (median or mean) and a measure of uncertainty (credible interval). Once we have the reliability distribution for each component, we use Monte Carlo integration to compute a system reliability distribution.

Figure 3-2 provides an illustration for combining component-level data for the system reliability estimate using MCMC. The top four figures represent different posterior distributions for components. The first and fourth components represent closed-form analytic solutions from which we would sample, while the second and third components represent posteriors obtained using MCMC. We repeatedly draw values from the distribution of each component using

MCMC. Each value is combined using Monte Carlo to give the system reliability estimate, based on the assumed series or parallel structure of the components in the system. The resulting estimate of the system reliability is shown in the bottom plot of Figure 3-2.

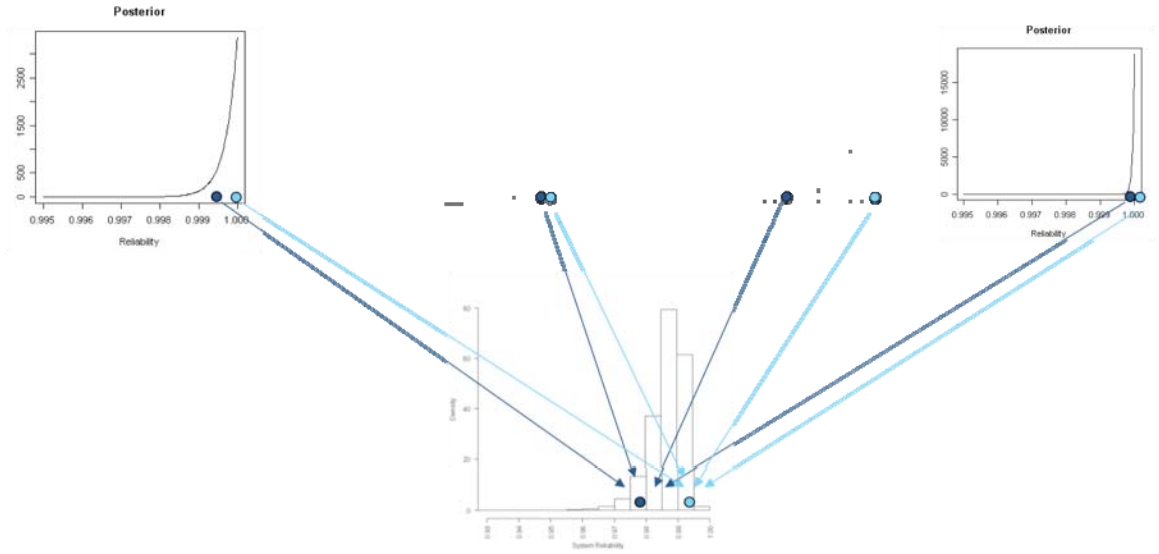

Figure 3-2. Combining component-level data for system reliability estimate.

The methodology of Bayesian inference applied directly to the subject area of reliability is detailed in many excellent texts including Martz and Waller (1982) and Hamada et al. (2008).

Data and Prior Distributions

We describe the data and form of the prior distributions used for some of the components in order of increasing complexity of the distributions for each block. We also present some sensitivity analysis for the priors. We consider the components J5, J7, J4, K14–K15–K16, and JK20 here. Components J6, K19, and K20 are similar to J5. Component J8 is assumed to have constant reliability of 1.0. All of these illustrate different aspects of the inference problem. We also present and discuss the negative-log gamma distribution (Lawrence and Vander Wiel 2006), a relatively new distribution in reliability that has some very useful properties.

Block J5: This is the simplest component because it fits into the standard Bayesian framework for binomial data. For this component, there were 3,513 tests, all resulting in success. There is no aging in this data. We use a binomial model for the success/failure data with a conjugate beta prior giving a beta posterior distribution. Figure 3-3 gives an illustration of the sensitivity of the prior for three priors that are commonly used with the binomial: a uniform prior, a Jeffreys prior, and an informative beta prior. For comparison, the median and 95% credible interval are given in Table 3-1. The differences in the posteriors are a reflection of the combination of the data and prior information. Depending on what experts believe to be true about the component reliability before the data is observed, when the analysis combines the data and prior, slightly different

results may be obtained. This emphasizes the importance of thinking carefully about what is known about the reliability outside of the data currently being considered to accurately reflect that knowledge. As the amount of data in the current study increases, the posterior becomes less dependent on the shape, center, and spread of the prior.

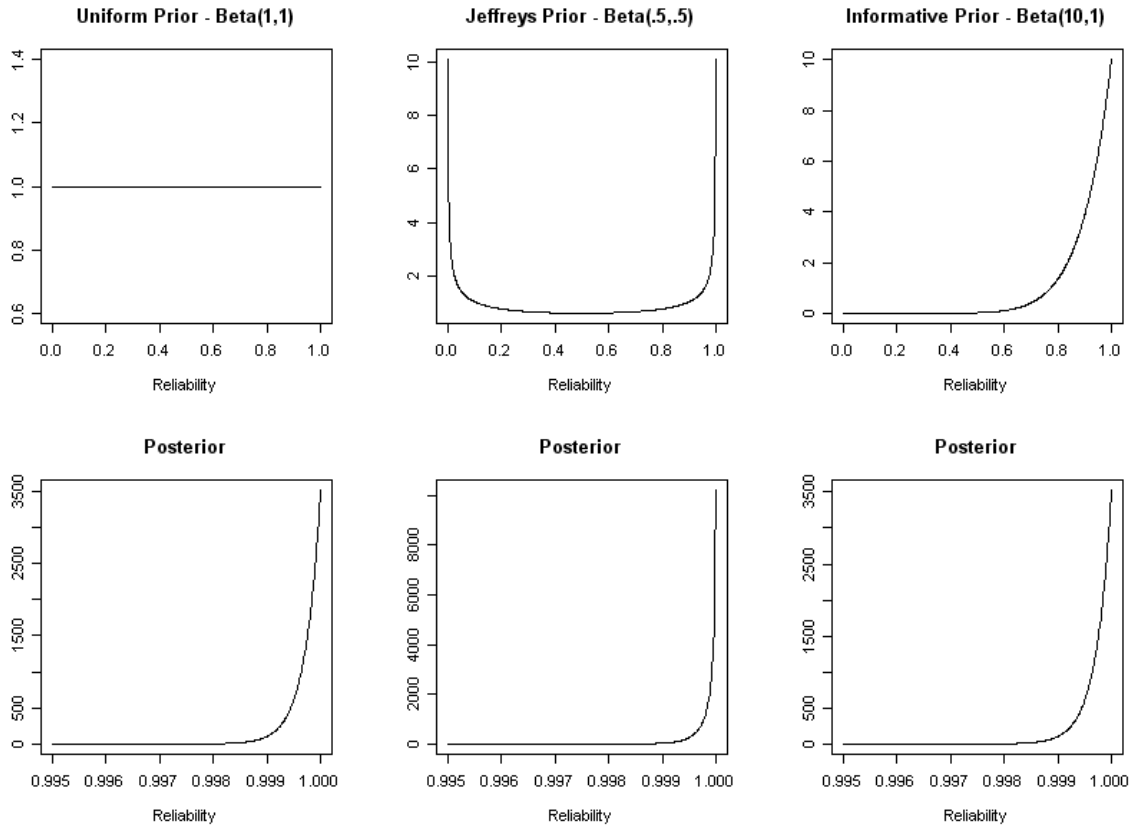

Figure 3-3. Three different priors (top row) and resulting posteriors (bottom row) for binomial data for component J5.

Table 3-1. Prior Distribution and Resulting Posterior Median and 95% Credible Intervals for Component J5.

Prior Distribution	Posterior Median	95% Credible Interval
Uniform(0,1)	0.999803	(.998995,.999993)
Jeffreys Prior	0.999935	(.999285,1.00000)
Beta(10,1)	0.999803	(.998954,.999993)

Blocks J6, K19, and K20: These blocks have binomial data and are analyzed similar to J5 using *Beta(1,1)* priors. The data for block J6 is 31484 tests, resulting in 31478 successes and 6 failures. The posterior median is 0.999820 and the 95% credible interval is (0.999629, 0.999930). The data for block K19 has 3338 tests, all resulting in success. The posterior median is 0.999792 and the 95% credible interval is (0.998896, 0.999992). The data for block K20 is 18,803 tests, resulting in 18,799 successes and 4 failures. The posterior median is 0.999752 and the 95% credible interval is (0.999455, 0.999914).

Block J7: Component J7 is composed of four components in series, J7A, J7B, J7C, and J7D. We discuss each component separately and then show how to combine the results for all of J7. The data used with J7 here is an expansion of the basic information on this event given in Chapter 1.

Components J7A and J7B: J7A consists of 383 variables measurements with a requirement that each measurement be in the interval (–4.5, 4.5). J7B consists of 468 variables measurements with a requirement that each measurement be in the interval (–3.8, 3.8). There are 383 tests that provide measurements of J7A and J7B, and 85 tests that measured J7B. In addition, 2,327 tests recorded pass/fail data that ensured that both J7A and J7B were within requirements. These include the 468 tests described above.

This combination of having both pass/fail and continuous measurement (variables data) on components is called multilevel data (cf., Wilson and Huzurbazar 2007).

For this data, we use normal distributions with mean μ_A and variance σ_A^2 for J7A and mean μ_B and variance σ_B^2 for J7B. We use noninformative priors on all the parameters such that we have flat priors on μ_A and μ_B and diffuse (1/variance) priors on σ_A^2 and σ_B^2. The posterior is given by

$$\frac{1}{\sigma_A^2 \sigma_B^2} \prod_{i=1}^{n_A} \frac{1}{\sigma_A} \exp\left(-\frac{1}{2\sigma_A^2}(x_i - \mu_A)^2 \right) \bullet \prod_{j=1}^{n_B} \frac{1}{\sigma_B} \exp\left(-\frac{1}{2\sigma_B^2}(y_j - \mu_B)^2 \right) \left[(\Phi(4.5, \mu_A, \sigma_A) - \Phi(-4.5, \mu_A, \sigma_A))(\Phi(3.8, \mu_B, \sigma_B) - \Phi(-3.8, \mu_B, \sigma_B)) \right]^{n_C} \tag{33}$$

where Φ is the standard normal cumulative distribution function and a term such as $\Phi(4.5, \mu_A, \sigma_A) - \Phi(-4.5, \mu_A, \sigma_A)$ gives the probability that the component J7A is within requirement. We use MCMC to sample from the posterior in Equation (2). For J7A and J7B together in series, the posterior distribution median is 0.9998 and a 95% credible interval is (0.9996, 0.9999). Figure 3-4 gives a histogram of samples from the joint posterior distribution of J7A and J7B.

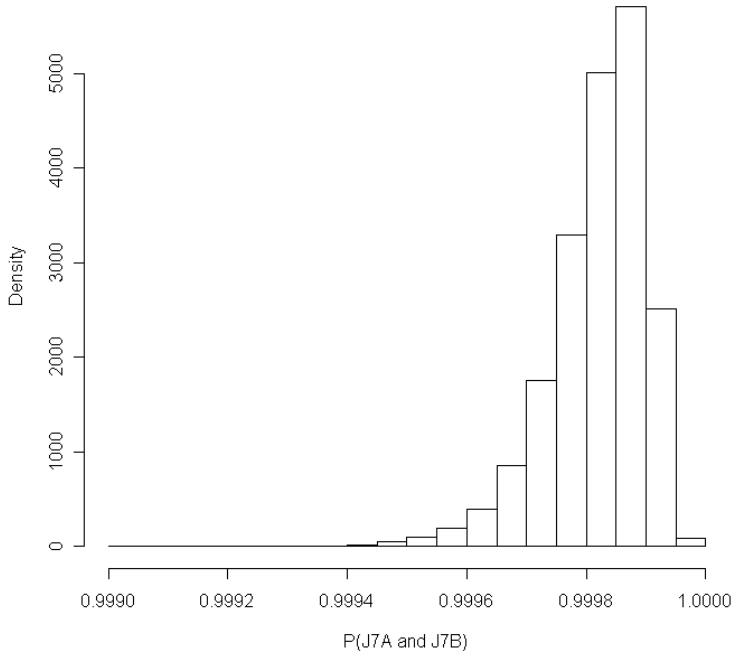

Figure 3-4. Histogram of samples from joint posterior distribution of J7A and J7B.

Component J7C: For this component, we have 15 variables measurements on J7C with a requirement that they be in the interval (–6.0, 6.0). These observations are independent of the other data. We assume that the data is normally distributed with mean μ and variance σ^2. We use a flat prior on μ and a noninformative (1/variance) prior on σ^2. The posterior is proportional to

$$\frac{1}{\sigma^2}\prod_{i=1}^{n}\frac{1}{\sigma}\exp\left(-\frac{1}{2\sigma^2}(x_i-\mu)\right) \tag{34}$$

Figure 3-5 gives a histogram of the data along with a histogram of samples drawn from the posterior distribution of Equation (3) using MCMC. The distribution is very skewed, with a posterior median of 1.0 and a 95% credible interval of (0.9999997, 1.0).

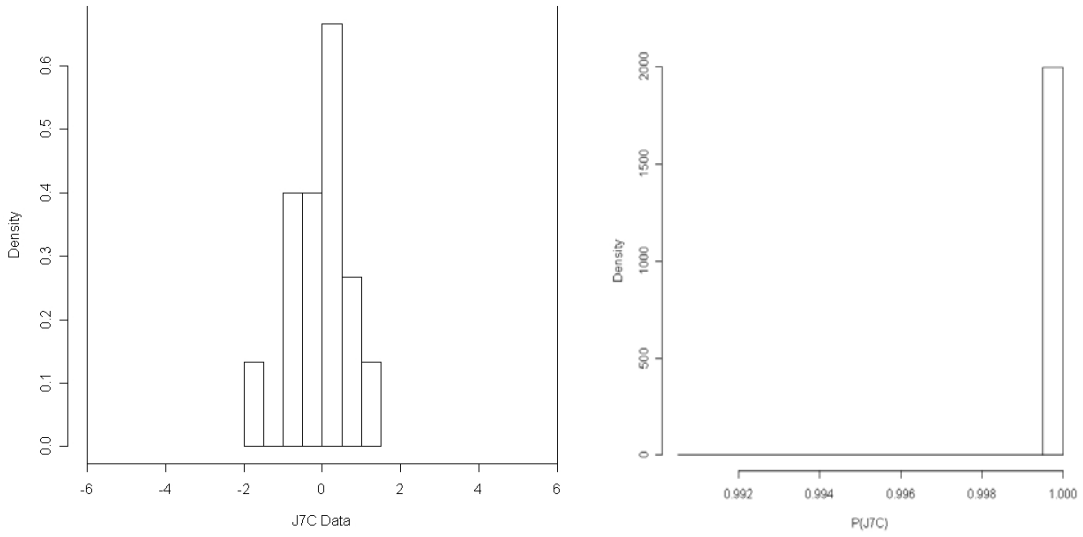

Figure 3-5. Histogram of data from J7C (left) and posterior samples (right).

Component J7D: There were no failures in 71,784 tests (trials). The total number of individual parts tested to obtain the trials data was 6,175. We used a negative log-gamma (NLG) (0.25,1) distribution for the prior.

The NLG distribution was introduced by Springer and Thompson (1967) specifically for problems in system reliability. Martz and Waller (1982) and Lawrence and Vander Wiel (2006) provide detailed explanation. The NLG distribution has the property that for components in series that have NLG priors, the system-level prior is Uniform(0,1). In our case, this means that the block prior is Uniform(0,1) and the prior on each success probability p_i is:

$$\begin{aligned} &-\log(p_i) \sim gamma(\alpha_i,1) \text{ where } \sum \alpha_i = 1 \\ &p_S = \prod p_i \\ &-\log(p_S) = -\sum \log(p_i) \sim gamma(1,1) \\ &\Rightarrow \quad p_S = Uniform(0,1) \end{aligned} \tag{35}$$

We use MCMC to sample from the posterior to give the posterior distribution samples in Figure 3-6. The posterior distribution median is 0.999993, and a 95% credible interval is (0.99972, 1.0).

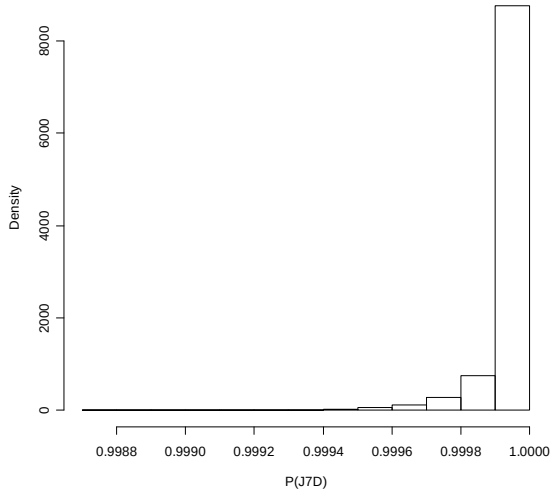

Figure 3-6. Histogram of posterior samples from J7D.

Block J7: We use Monte Carlo to combine the posterior samples from the four components in series: J7A, J7B, J7C, and J7D. We take a product of the joint draws of (J7A, J7B) and marginal draws of J7C and J7D. The posterior samples are shown in Figure 3-7. The distribution median is 0.9998, and the 95% credible interval is (0.9995, 0.9999).

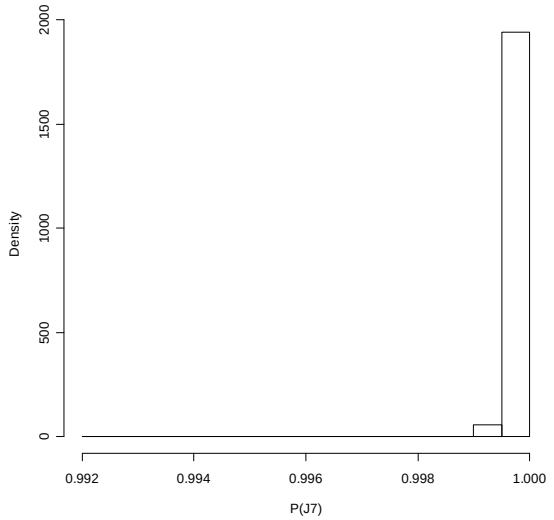

Figure 3-7. Posterior samples for the four-component series system represented by J7.

Block J4: This is composed of five components in series, J4A, J4B, J4C, J4D, and J4E. J4A, J4B, and J4D are assessed as series systems with data from all three components combined. They are judged to be "similar enough" to be evaluated jointly. All three have the following events:

E1: 0 failures in 200,000 tests
E2: 0 failures in 200,000 tests
E3: 0 failures in 1,000 tests.

In addition, J4A and J4B have an additional failure event E4: 1 failure in 516 tests. We calculate p1, p2, p3, p4 corresponding to failure events (E1,…,E4) using the NLG(1/β,1) prior distribution and binomial data. The NLG is used so that J4 has a uniform prior distribution. The posterior samples are given in Figure 3-8. J4A and J4B have the same distribution. The distribution median is 0.9984 with a 95% credible interval of (0.9925, 0.9999). For J4D, the distribution median is 0.9999982, and the 95% credible interval is (0.9991, 1.0).

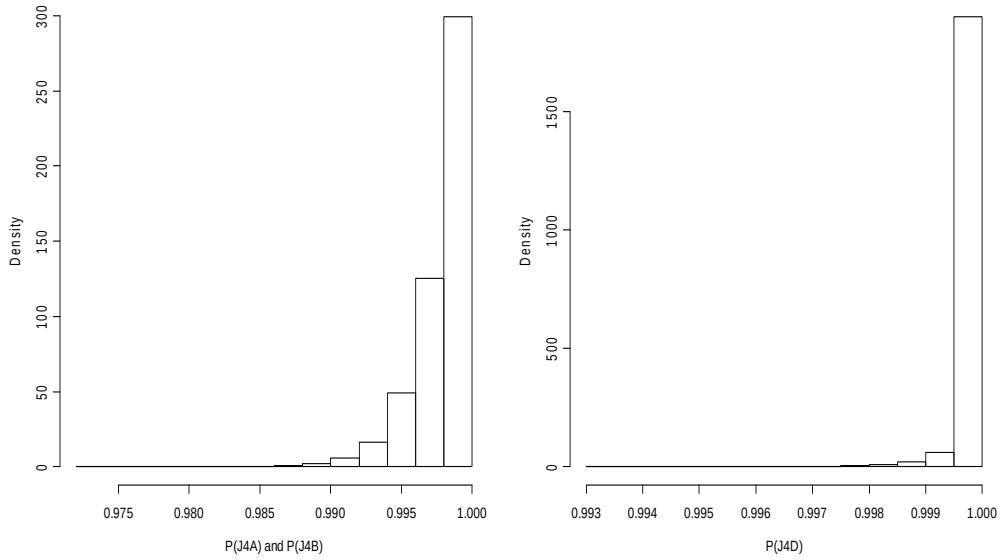

Figure 3-8. Posterior sample histograms for J4A (and same for J4B [left]) and J4D [right]).

Component J4C: This component had one failure in 5,000 tests. The approach is to find p_C using an NLG(1/13,1) prior along with binomial data. The histogram of posterior samples is given in Figure 3-9 where the distribution median is 0.9998 and the 95% credible interval is (0.9992, 0.999993).

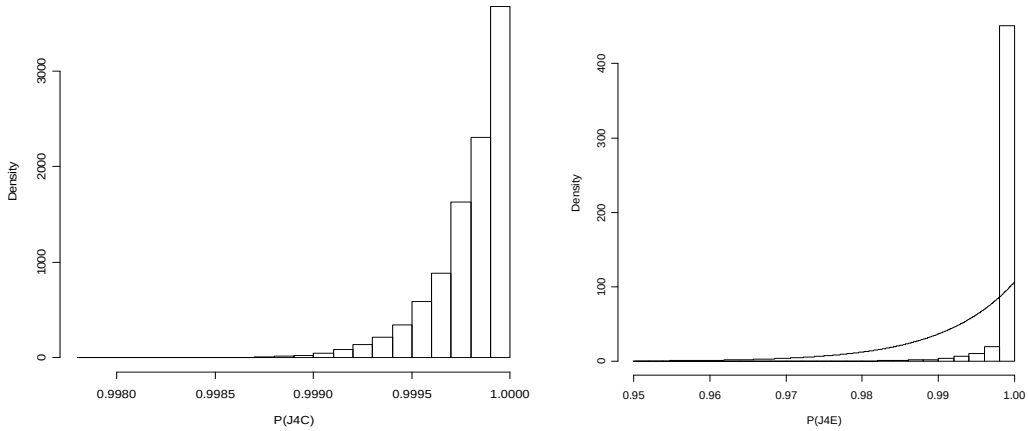

Figure 3-9. Posterior samples for J4C (left) and J4E (right). The solid line on the J4E is the posterior with a uniform prior.

Component J4E: Component J4E had 106 successful tests with no failures. p_E is calculated using an NLG(1/13,1) prior along with binomial data. The posterior is presented in Figure 3-9 along with some sensitivity analysis using a uniform prior (solid line in Figure 3-9, right). With the NLG, the distribution median is 0.999998 and a 95% credible interval is (0.9914, 1.0). For the uniform prior, the distribution median is 0.9935, and the 95% credible interval is (0.9661, 0.9998).

Block J4 Results: The five-component series system is a product of 13 probabilities, $(p_1p_2p_3p_4)(p_1p_2p_3p_4)(p_C)(p_1p_2p_3)(p_E)$. We use Monte Carlo to combine the five components, six distinct probabilities together. The distribution on J4 has a median of 0.9960 and a 95% credible interval of (0.9818, 0.9996). Posterior samples from J4 are given in Figure 3-10.

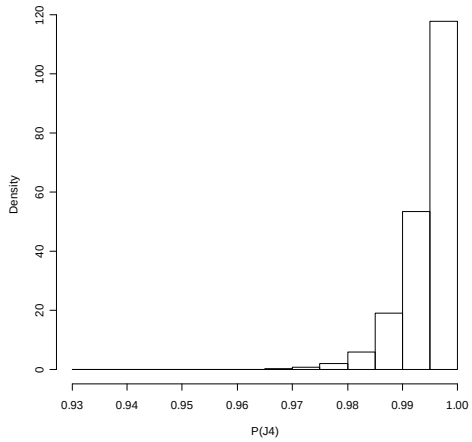

Figure 3-10. Histogram of resulting distribution on J4 by combining posterior samples on components J4A–J4E.

Blocks K14, K15, and K16: These components are distinct but are tested together so that we do not know which one failed. We observe 1 failure in 4,132 tests. The failure allocation with K14, K15, K16 is 4:4:1. The probability that the system works is $p_S = p_1p_2p_3$. We have binomial data with success probability p_S. We use an NLG prior on (p_1,p_2,p_3) with $\alpha_1 = \alpha_2 = 4/9$ and $\alpha_3 = 1/9$, which matched the gamma prior means to the failure event ratio. This induces a Uniform(0,1) prior on at the block level.

The posterior distribution median is 0.9999415 with a 95% credible interval of (0.9991630, 1.0) and is shown in Figure 3-11.

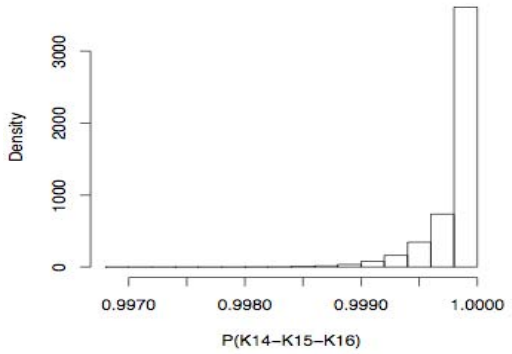

Figure 3-11. Joint posterior samples for K14, K15, K16.

Block JK20: This block represents a subsystem with components C_1 and C_2, each of which produces an amplitude, A_1 and A_2, respectively. The reliability in this case is age-dependent through the amplitude. Figure 3-12 shows a block diagram of the subsystem.

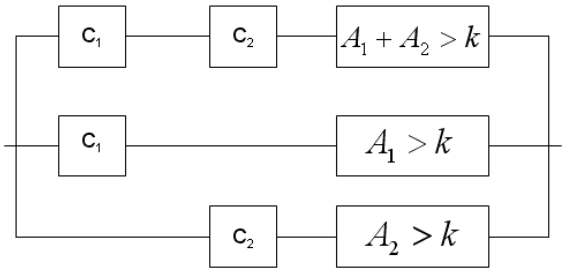

Figure 3-12. Block diagram for JK20.

We assume that C_1, C_2 have the same reliability distribution and that $\text{Log}(A_1)$ and $\log(A_2)$ are i.i.d. $N(a+bt_i, \sigma^2)$. The data on C_1 and C_2 has 100 failures in 2,500 trials. We model reliability of C_1, C_2 with a Beta(1,1) (Uniform) prior, which gives a Beta(2401,101) posterior. $\text{Log}(A_1)+\log(A_2)$ are i.i.d. $N(2(a+bt_i), 2\sigma^2)$. We simulated 400 "ages" from Gamma(1.4, 0.27) so that $t_1,\ldots,t_{400}$ have a median = 4, and a 99th percentile = 20. We generated observations from an $N(a+bt_i, \sigma^2)$ with a = 29.22, b = –0.1204, σ = 0.1826. We used diffuse gamma priors on a, b and inverted gamma on σ^2. The posterior probabilities of interest are $P(A_1>\text{age cutoff})$ and

$P(A_1+A_2>\text{age cutoff})$. Figure 3-13 gives a plot of the amplitude changing over time and the posterior samples from block JK20. Figure 3-14 gives a plot of the system reliability over time and a plot of the posterior at age = 130 years.

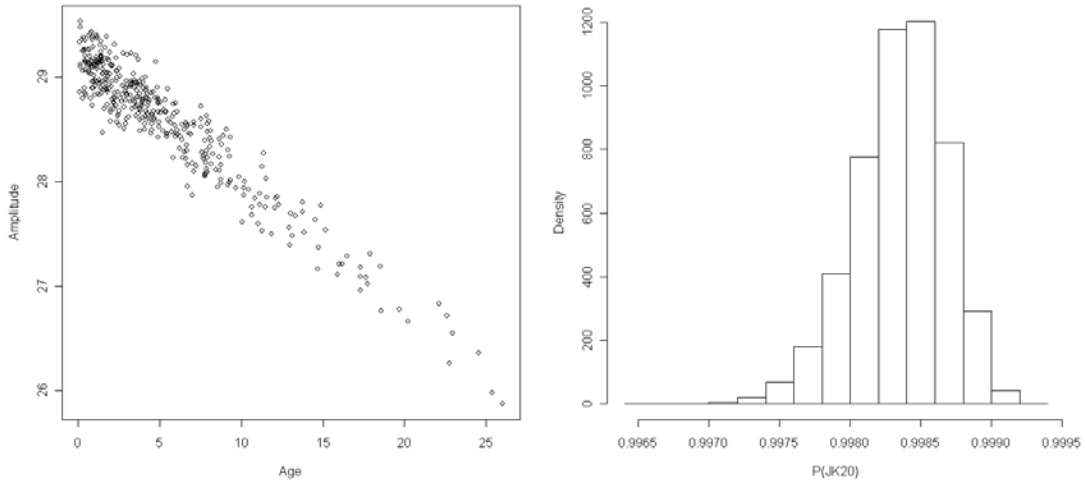

Figure 3-13. Amplitude as function of time (left) and posterior on JK20 at age 0 (right).

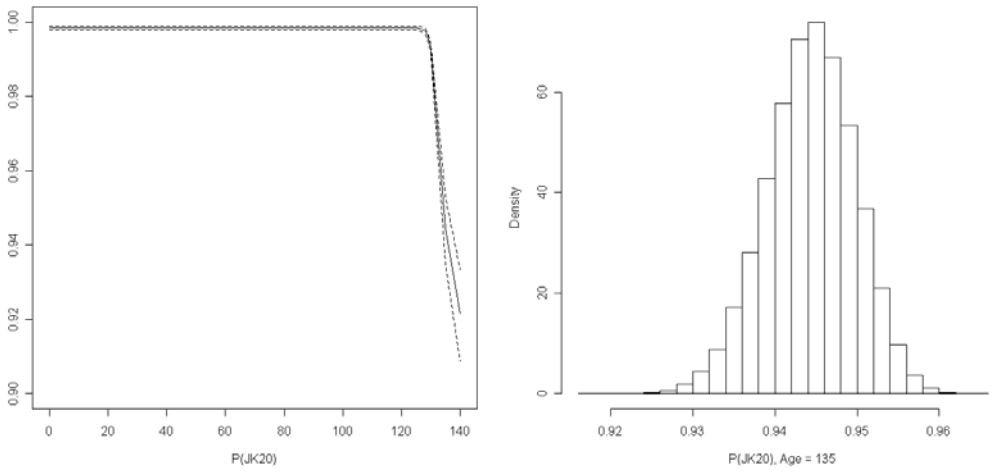

Figure 3-14. System reliability over time (left) and posterior at age 130 years (right).

Block JE1: This block is the node that captures the epistemic uncertainty. In the first analysis (left-side results of Figure ES-1), we assume that it makes no contribution to the variability of the system. This corresponds to assuming a reliability distribution of "1" for this component. In the second (right side of Figure ES-1) we assume that there is a hypothesized failure mode above a certain stress level for which we have no data. The reliability is assumed to be not time-dependent. While no data was available for this block's analysis, a probability distribution is chosen to reflect the a priori belief that there is a 50% chance of a 0.5% problem, and a 5% chance of a 1% problem. The distribution that captures this assumption is a Beta(861.2,4.655). Note this is an extension of the basic problem as laid out in Chapter 1.

Combining Component-Level Data

Once we have a distribution to estimate the reliabilities for all components of the system, we can combine these distributions using Monte Carlo to obtain an overall distribution to estimate the system reliability. Note that not all component reliabilities have been estimated independently (e.g., K14, K15, K16). Thus, we must sample from the joint distribution of the nonindependent components (instead of their marginal distributions).

If we assume that "JE1" has reliability of "1" and include no additional uncertainty for "J4E," then we obtain the following reliability estimates for the system. The distribution median is 0.9941. The resulting quantiles are

95%:	0.9972
5%:	0.9852.

Figure 3-15 gives the system reliability for the second scenario, where we have included some uncertainty in the estimates of both "JE1" and "J4E." Then the distribution median is 0.9880. The resulting quantiles are

97.5%:	0.9941
95%:	0.9935
5%:	0.9767
2.5%:	0.9734.

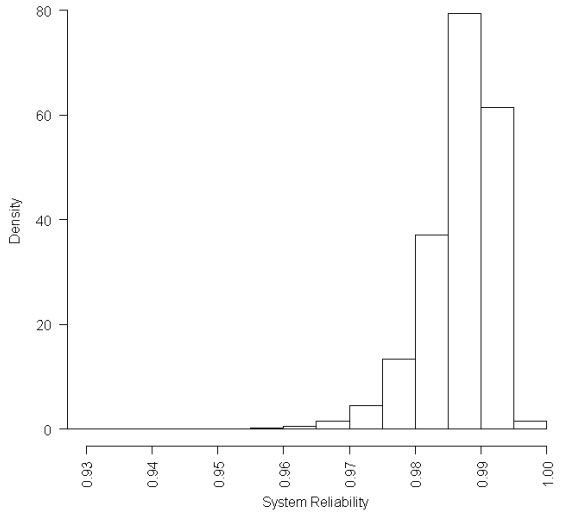

Figure 3-15. System reliability for block diagram of Figure 3-1.

We can also attribute the uncertainty in the inputs to uncertainty in the output using posterior draws to approximate the largest contributors to approximate the expected variability of the system reliability with or without the component reliability uncertainty $E[Var(X_i|X_{-i})]$. Figure 3-16 displays this for the system at age = 0 for the second scenario with included uncertainty for both "JE1" and "J4E" in a Pareto bar plot for variance contribution rather than counts. By ordering the component contributions to the overall uncertainty in the system reliability estimate, we are able to determine the relative contribution of the components to the precision of our estimates.

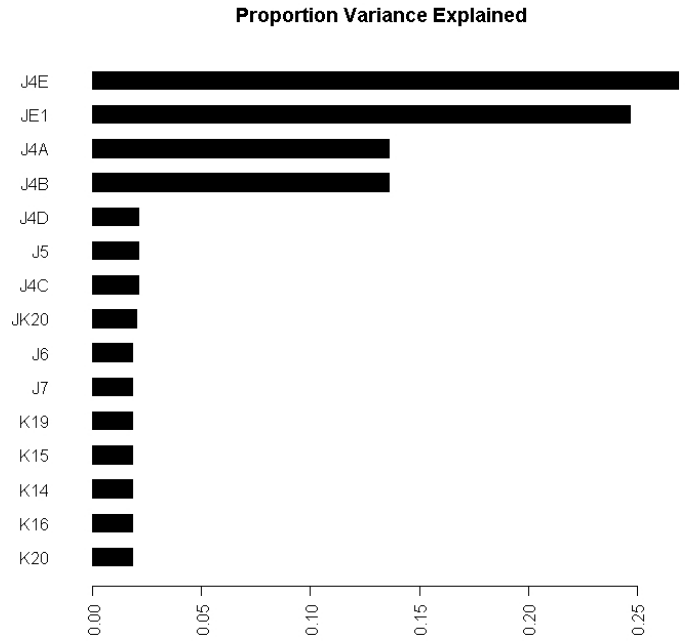

Figure 3-16. Uncertainty attribution for output uncertainty.

The largest contributors to variance are J4E and JE1, as shown in Figure 3-17.

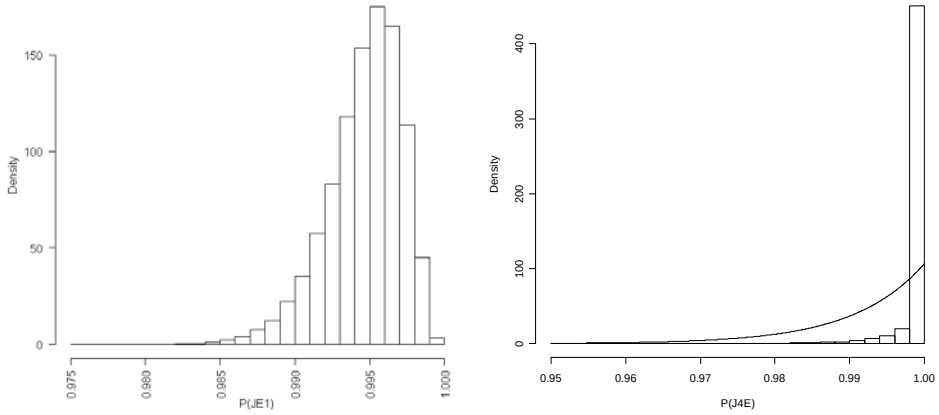

Figure 3-17. Largest contributors to variance (J4E and JE1).

Figure 3-18 shows the overall system reliability as a function of time. An implicit assumption of the current model for components with no aging trend is that the component reliabilities can be predicted beyond the observed ages with no change in this non-aging assumption.

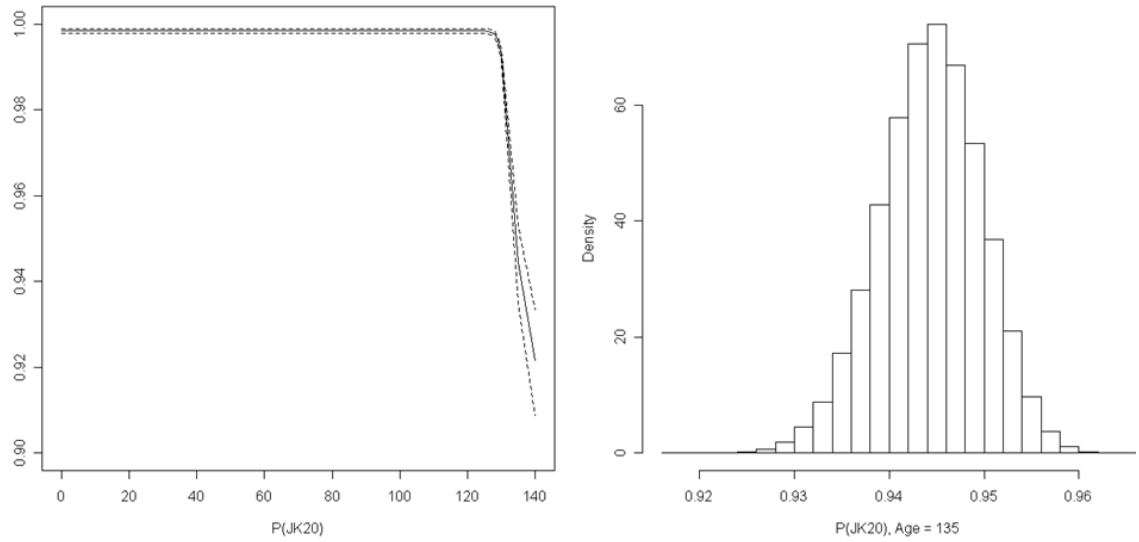

Figure 3-18. JK20 reliability distribution as a function of age with histogram of reliability at age 135 years.

4. COMPARISONS AND OBSERVATIONS

The previous sections provide a proof of concept for two different approaches for estimating reliability and its associated uncertainty in a sample system. This section briefly explores the similarities and differences both in the formulation and execution of the two methods.

Sensitivity to Zero-Failure Case Assumptions

Although the two approaches have significant conceptual differences, in the case study explored here the two can give closely comparable results. Both methods prove to be sensitive to how they handle zero-failure cases. This sensitivity can be much larger than the differences in results between Classical and Bayesian formulations.

Figure 4-1 compares 90% confidence/credible intervals for the Classical and Bayesian approaches.

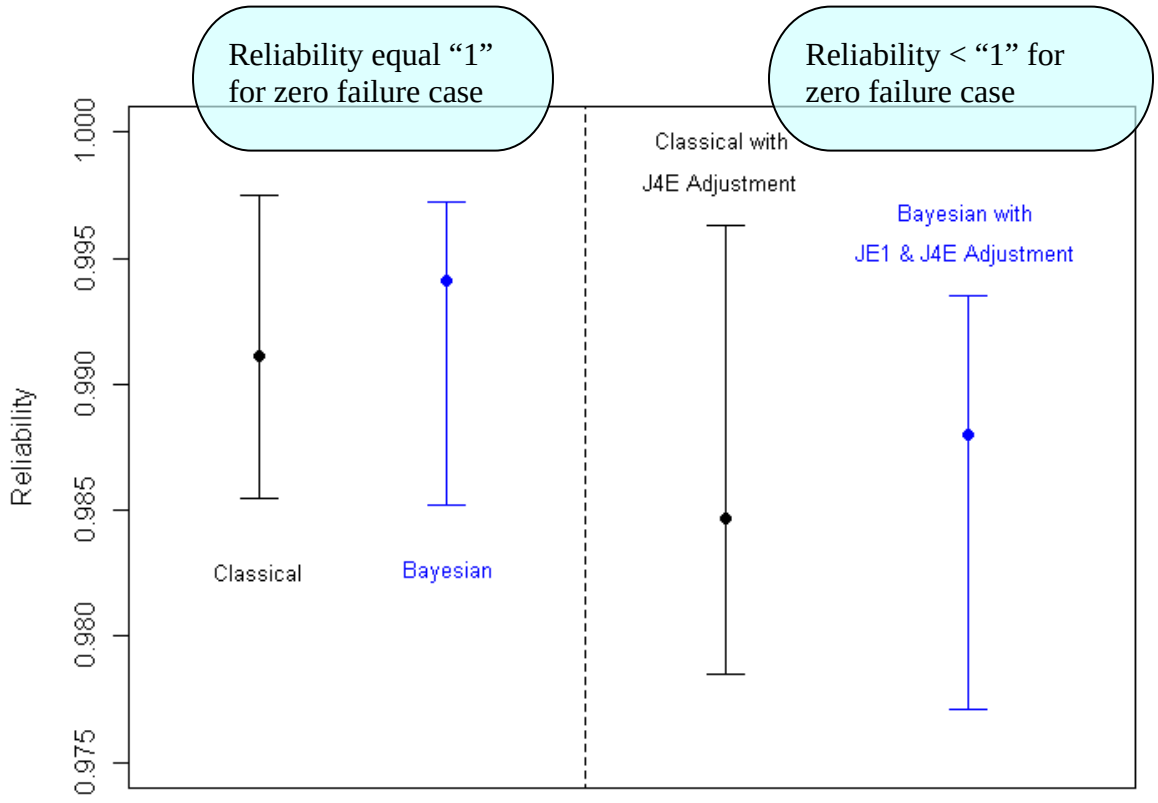

Figure 4-1. Confidence/credibility interval comparison.

Assume Reliability = 1 for Zero-Failure Case

The left side shows the Classical and Bayesian approaches using a reliability of "1" for both component J4E that has zero failures and for knowledge uncertainty event JE1. The results in the Classical and Bayesian approaches in this case are almost identical: the Classical 90% confidence interval is (0.9855, 0.9975) centered at 0.9911; the Bayesian 90% credible interval is (0.9852, 0.9972) with a median of 0.9941. The width and placement of the two intervals is quite similar with the point estimate of the Classical method being slightly lower than the Bayesian estimate. Note that in this case of zero failures, when the Classical approach assumes a reliability of "1" it naturally associates this with no uncertainty whereas the Bayesian approach would more naturally apply the flexibility to account for the associated uncertainty through a prior distribution.

Assume Reliability Not Equal to 1 for Zero-Failure Case

The right side of Figure 4-1 explores another pair of alternatives for the zero-failure cases. If we select the 50% upper confidence limit for J4E, the Classical approach estimates a lower mean reliability, and a wider 90% interval. The second (labeled "Bayesian with JE1 & J4E Adjustment") estimates system reliability using the Bayesian approach and incorporates uncertainty for both J4E and JE1. The uncertainty for J4E is estimated by using a diffuse prior, and the uncertainty for JE1, which represents a hypothesized unknown failure mode, is summarized by a beta distribution formulated based from expert elicitation. The uncertainty of the JE1 component is not included in the Classical estimate; hence these two results are not directly comparable. Because the Bayesian interval contains this extra component, the bounds are somewhat lower than the Classical ones. However, the overall point estimate of system reliability remains higher than the Classical approach by an amount similar to that in the first comparison.

Contributors to System Uncertainty

Table 4-1 compares the largest contributors to system uncertainty. These results draw from Table 2-3 and Figure 3-16. The "Left" and "Right" analyses correspond to those discussed for Figure 4-1. Note that the percentages of the uncertainty explained are scaled differently, since the widths of the intervals differ between approaches. While both the Classical and the Bayesian approaches produce an ordering that is roughly comparable, there are obvious differences. Both the details on what the contributors represent and the scales of measurement contribute. The full nature of the differences remains to be explored but some general observations can be made on individual components.

- The JE1 event used different models in the two computations. The Classical computation assumed no uncertainty and no impact on reliability here. On the other hand, the Bayesian model allows for the inclusion of uncertainty through a prior that matches specified assumptions about the expert assessment of the likelihood of potential problems from this component.

- The J4E event only enters in the "Right" analyses. The Classical calculation used the 50% upper confidence level as the best estimate of the failure probability associated the relatively small sample size (106 trials) with considerable uncertainty. The Bayesian approach of applying an NLG prior is updated by the observation of 0 failures in 106 trials associated less uncertainty. As noted in Chapter 3, this is a place where the Bayesian calculation shows considerable sensitivity to assumptions. For an NLG(1/13,1) prior, which was used for the calculation reported above, a 95% credible interval for J4E would be (0.9914, 1.0). For a uniform prior (which assumes that reliabilities between 0 and 1 are all assumed equally likely), the interval would be (0.9611, 0.9998). Note that the assumed user knowledge about the reliability of the system for these two priors is very different (ranging from a belief that reliability is centered around 0.95 versus centered around 0.5). Since these priors represent very different assumptions about the state of the component, we would hope that they would have an impact on our post-analysis summaries of the component reliability.

Table 4-1. Largest Contributors to Uncertainty.

Classical Model			Bayesian Model		
Contributor	**Contribution (R=1 for 0 failure cases)**	**Contribution (R < 1 for 0 failure cases)**	**Contributor**	**Contribution (R=1 for 0 failure cases)**	**Contribution (R < 1 for 0 failure cases)**
	N/I	N/I	JE1 event	N/I	25%
$(1-Y_6)$ – J4E event	N/I	64%	J4E event	N/I	27%
$(1-Y_4)^2$ – J4A and J4B events	56%	20%	J4A, J4B	29%	14%
JK20 event	25%	9%		4%	2%
$(1-Y_3)^3$ – J4A, J4B and J4D events	18%	6%	J4D	4%	2%
others	<1%	<1%		<3%	<2%

N/I = not included

- The contributed uncertainty from J4A and J4B events came next for both approaches. There is reasonable alignment here, but note the Classical and Bayesian approaches are measuring the uncertainty associated with somewhat different things. The Classical value gives the contribution associated with data source Y_4, which is one contributor to J4A and J4B. The Bayesian deals with the reliability contribution from J4A and J4B directly. This reflects the differences in the approaches themselves. Classical approaches use probability to measure randomness associated with data and data sources. Bayesian approaches measure the same quantities and in addition use probability distributions to measure uncertainties in knowledge about underlying parameters.

- The JK20 event also shows some differences. The Classical calculation is for system end of life of 130 years while the Bayesian calculation was done for both beginning of life (0 year) and at end of life (30 years). The Classical calculation includes the uncertainties involved in the considerable extrapolation of the data illustrated in Figure 3-13. The Bayesian calculation handles continuous aging and also explores uncertainties as part of the sensitivity study reported in Figures 3-14 and 3-18. It should also be noted that the Classical calculation shows considerable sensitivity to the specific lifetime: an extrapolation to 129.5 years show results much closer to those for the Bayesian uncertainty calculation at 130 years. In both cases, the assumption that the model form of linear degradation towards a known specification limit is central to the projection of reliability. If another failure mode or the pattern of the degradation changed beyond the range of observed data, then the reliability estimates of both approaches would be invalid.

- As was the case for the Y_4/J4A and J4B discussion, the uncertainties associated with Y_3 and J4D shown on the last of Table 4-1 measure somewhat different things.

Comparison and Contrasts Between Approaches

Separate from these specific results, some general comparisons and contrasts can be made about the approaches.

Philosophically, there are, of course, the familiar, if considerable, differences. Interval estimates in both cases rest on a statement of the form

$$\text{Prob}(L < \text{Reliability} < U) = 0.90 \qquad (36)$$

but the handling of that statement is very different. The Bayesians treat the reliability as a random variable and compute L and U based on its distribution. The resulting interval is called a credible interval. The frequentists treat L and U as random variables whose distribution depends on the unknown (but nonrandom) reliability. As noted in the discussion of event J4E, the breadth of the uncertainties being captured by the concept of "probability" is different as well.

Both approaches embed judgments that can greatly influence the results. This was clearly illustrated in the discussion of the J4E event but applies more generally in other assumptions and approximations involving statistical distributions.

As with the J4E event, the Bayesian prior distributions seek to capture what experts know, with specific distributional choices being typically used. Classical approximations come at the end of the calculation where the moments of R_{SNL} need to be equated with some distribution. Here an equivalent binomial was used. And with that choice, the confidence interval bounds given by Equation (31) only give an approximate solution to Equation (36). Other distributional approaches might be explored in follow-on studies, such as use of the chi-square distribution associated with the asymptotic theory behind the likelihood ratio test. In any case, the sensitivity of results to all such choices, judgments, and approximations need careful review before too much credence is put in the specific results.

These results illustrate that the two approaches seek to reflect somewhat different sources of uncertainties. The Classical approach incorporates and propagates sampling uncertainties through distributional approximations. It does not include other knowledge-based sources of uncertainty. These must be handled via a larger risk-based structure as discussed in Ringland et al. (2009). The Bayesian approach allows for expert knowledge about each component to be incorporated via a prior and propagates uncertainties using Monte Carlo simulation.

Both approaches start from a small number of basic principles but then require a fair amount of mathematical or computational machinery to execute. In the Classical case, much of the complexity involves the analytic manipulation of the equations. For more complex problems than the one here, however, some of this might be done numerically (e.g., numerical computation of the derivatives needed for the mean and variance expansions). In the Bayesian case, more of the analysis was done numerically, and the underlying use of MCMC and other simulation and numerical integration techniques are both sophisticated and computation-intensive.

Two additional issues with the Classically based SNL reliability estimator should also be pointed out.

First, the uncertainty calculation for R_{SNL} depends on values that would be used if there are zero failures for the various subsystems, e***ven when one or more failures has been seen and those values are not active.*** That is part of the structure of Classical (Neyman-Pearson) philosophy where probabilities represent repeated frequencies over conceptual repetitions of the entire test/surveillance history. It is often said that the zero-failure values are not relevant for mature systems because most components will have seen failures. From the perspective of Classical statistical uncertainty calculations based on Neyman-Pearson philosophy, that is not true, although the impact is reduced with more data and more observed failures. In a sense, the situation resembles the Bayesian situation where the influence of the prior distribution decreases as more data is available.

Second, the use of R_{SNL} itself deserves re-examination. It is known to be a biased estimator because of the special handling of zero-failure results for individual subsystems. As shown in Ringland (2008), R_{SNL} can have lower mean square error (a frequently used measure of goodness in Classical statistics) than an estimator without special handling of zero-failure cases if system unreliability is the result of subsystem unreliability localized to one or two such subsystems. If three or more subsystems are significant contributors, R_{SNL} is not necessarily superior, and can be much worse.

Some concluding observations about the Bayesian analysis are given below.

- The Bayesian approach requires that expert knowledge be incorporated into the analysis. While there is considerable flexibility about the specificity and the nature of the information captured in the prior, there is a requirement to consider what is known about the reliability of the component outside of the data currently included in the analysis. Diffuse priors can be used if the expert knowledge is not specific, and the impact of the prior is dependent on the amount of data in the analysis. For a component with little data, the impact of the prior can be substantial. Since this study was a proof of concept, we

primarily selected diffuse priors because expert elicitation for this fictitious system was not available. In a real application, considerable time would be spent on appropriate prior selection to incorporate expert judgment.

- In the above analysis, since the analysis represents a fictitious system, we assumed that little was known outside of the data available. For each block, it was assumed that a uniform distribution from [0,1] was appropriate to summarize what was known. This subjective choice was made to avoid inserting artificial outside knowledge into the analysis, in an effort to make the two approaches most comparable. In general, it would be typical to have expert opinion that would make these priors less diffuse, and more accurately reflect what is known about the system and its components. This prior may be inherently pessimistic, since it implies that a reliability of less than 0.5 is as equally likely as a reliability of more than 0.5. This assumption was then translated to information at the sub-block levels (in the cases of J7 and J4 where multiple failure modes or subcomponents were involved). The NLG model allows for priors to be constructed at the sub-block level, while preserving the desired prior characteristics at the block level.

For this proof-of-concept case study, our focus is on demonstrating that these types of calculations can be performed on complex systems rather than aiming for a one-to-one comparison between the Classical and Bayesian approaches. Still, we were gratified by the degree to which the results were similar. This is only a first step toward gaining a scientific consensus on methods. More work would be required to extend these to a proper decision framework that is not overly simplified. In addition, to appropriately reflect the entire understanding of a real system, more emphasis would be placed on data acquisition and how to best capture other sources of knowledge from experts into the priors in the Bayesian method.

5. REFERENCES

Anderson-Cook, C.M., T.G. Graves, and M.S. Hamada, 2008, Resource Allocation: Sequential Design for Analyses Involving Several Types of Data, *IEEE Xplore Proceedings* from IEEM Singapore 2008.

Anderson-Cook, C.M., T.G. Graves, and M.S. Hamada, 2009, Resource Allocation for Reliability of a Complex System with Aging Components, *Quality and Reliability Engineering International* (in press).

Berger, J., 1993, *Statistical Decision Theory and Bayesian Analysis*. Springer, New York, NY.

Diegert, K.V., 2006, The Expression of Variability and Uncertainty in Reliability Assessment, PowerPoint presentation, February 11, 2006, Sandia National Laboratories.

Gelman, A., J. Carlin, H. Stern, and D. Rubin, 1995, *Bayesian Data Analysis*. Chapman & Hall/CRC Press, Boca Raton, FL.

Hamada, M.S., A.G. Wilson, C.S. Reese, and H.F. Martz, 2008, *Bayesian Reliability*. Springer, New York, NY.

Huzurbazar, A.V., C.M. Anderson-Cook, A.G. Wilson, and Q. Fatherley, 2009, *Reliability Uncertainty Aggregation Case Study for the B-61*. Los Alamos National Laboratory Technical Report, LA-UR-09-00172. Los Alamos National Laboratory, Los Alamos, NM.

Johnson, N.L., and S. Kotz, 1969, *Discrete Distributions*. John Wiley and Sons, New York, NY.

Lawrence, E., and S. Vander Wiel, 2006, *New Priors for Complex System Reliabilities and Trends*. Los Alamos National Laboratory Technical Report, LA-UR-06-5402. Los Alamos National Laboratory, Los Alamos, NM.

Martz, H., and R. Waller, 1982, *Bayesian Reliability Analysis*. Wiley, New York, NY.

Ringland, J.T., 2008, Early Production Reliability Calculations (MRRP Action Item 24), memo dated May 29, 2008, in response to an action raised in the December 2007 Methodology Reliability Review Panel, Sandia National Laboratories.

Lorio, J.F., K.V. Diegert, M.A. Dvorack, Q.M. Fatherley, M.J. Mundt, J.T. Ringland, and R.M. Zurn, 2009, *Prioritizing Surveillance Projects – A Risk Based Approach,* Draft SAND Report. Sandia National Laboratories, Albuquerque, NM..

Springer, M., and W. Thompson, 1967, Bayesian Confidence Limits for the Reliability of Cascade Exponential Subsystems, *IEEE Transactions on Reliability*, Vol. R-16, pp. 86–89.

Taylor, Barry N., and Chris E. Kuyatt, 1994, *Guidelines for Evaluating and Expressing the Uncertainty of NIST Measurement Results*, NIST Technical Note 1297, Physics Laboratory, National Institute of Standards and Technology, U.S. Department of Commerce. Available on line at http://physics.nist.gov/Pubs/guidelines/cover.html.

Wilson, A.G., T.G. Graves, M.S. Hamada, and C.S. Reese, 2006, Advances in Data Combination, Analysis and Collection for System Reliability Assessment, *Statistical Science*, Vol. 21, pp. 514–531.

Wilson, A.G., and A.V. Huzurbazar, 2007, Bayesian Networks for Multilevel System Reliability, *Reliability Engineering and System Safety*, Vol. 92, pp. 1413–1420.

DISTRIBUTION LIST

Distributed electronically

1	MS A109	Los Alamos National Laboratory Attn: Thomas Zocco Enhanced Surveillance Campaign Program Manager Weapons Engineering Technology Division Los Alamos, NM 87545
1	MS A122	Los Alamos National Laboratory Attn: Charles Hills W-9 Surveillance Oversight Los Alamos, NM 87545
1	MS P918	Los Alamos National Laboratory Attn: Eric Mas Weapons Physics Los Alamos, NM 87545
1	MS A115	Los Alamos National Laboratory Attn: Patty Buntain W-1: B-61 Los Alamos, NM 87545
1	MS A114	Los Alamos National Laboratory Attn: Pat Garcia W-4: W88 Los Alamos, NM 87545
1	MS P362	Los Alamos National Laboratory Attn: Frances Knudson STBPO-RL: Research Library Los Alamos, NM 87545
1	MS A114	Los Alamos National Laboratory Attn: Bill Sole Los Alamos, NM 87545
1	MS A115	Los Alamos National Laboratory Attn: Rick Mooday Los Alamos, NM 87545

1	MS F644	Los Alamos National Laboratory Attn: Mark Anderson Los Alamos, NM 87545
1	LLNL	Lawrence Livermore National Laboratory Attn: William McLean, L-125 Livermore, CA 94550
1	MS0175	M. A. Dvorack, 4225
1	MS0447	C. A. Post, 2111
1	MS0447	J. F. Lorio, 2111
1	MS0483	S. L. Flicker, 2112
1	MS0478	J. F. Arfman, Jr., 2138
1	MS0828	M. Pilch, 1551
1	MS0828	J. R. Red-Horse,1544
1	MS0829	K. G. Pierce, 415
1	MS0829	J. M. Sjulin, 415
1	MS0829	E. V. Thomas, 415
1	MS0829	S. V. Crowder, 415
1	MS0830	K. V. Diegert, 413
1	MS0830	M. J. Mundt, 413
1	MS9007	R. M. Zurn, 8205
1	MS9007	R. L. Bierbaum, 8205
1	MS9007	J. T. Ringland, 8205
1	MS9013	J. M. Baldwin, 8231
1	MS9014	D. M. Skala, 8238
1	MS9154	L. R. Carrillo, 8237
1	MS9158	P. T. Boggs, 8961
1	MS9158	M. Grace, 8961
1	MS0899	Technical Library, 9536 *(electronic copy)*


Sandia National Laboratories